

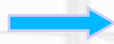


Decameter pulsar/transient survey of Northern sky

V. Zakharenko, I. Kravtsov, I. Vasylieva,
O. Konovalenko, O. Ulyanov,
A. Shevtsova, A. Skoryk, V. Kolyadin

Challenges and advantages of observing pulsed signals at low frequencies

1. Scattering



$$\propto f^{-4.4} \text{ (Kolm)}$$

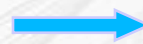
$$\propto f^{-4.0} \text{ (norm)}$$



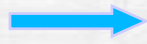
For frequencies 25 MHz and 1 GHz

$$(f_1/f_2)^{-4.4} = (25/1000)^{-4.4} \approx 10^7 \quad !$$

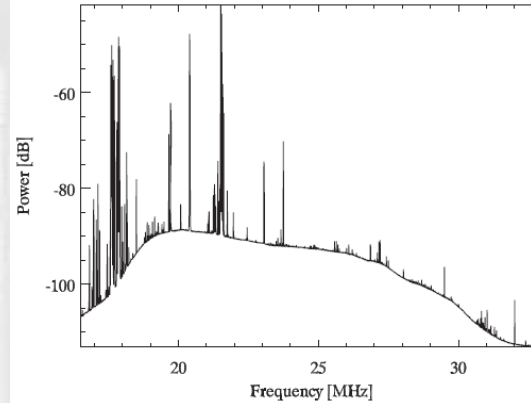
2. RFI (70-80 dB above background)



3. Galactic background



$$\propto f^{-2.5}$$

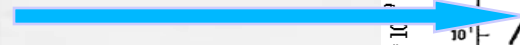


4. Dispersion delay



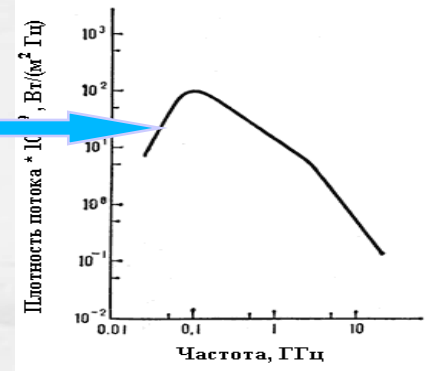
$$\Delta t = \frac{10^{16} \cdot DM}{2.410331} (f_{\min}^{-2} - f_{\max}^{-2})$$

5. Low-frequency slope of pulsar flux density



6. Low absolute bandwidth and pulse width

$$\Delta \tau, \Delta f$$



Until 2010, only a dozen pulsars were known in decameter wavelength

Decameter pulsar census with UTR-2:

[Zakharenko et al., 2013, MNRAS, 431, 3624]

- 74 pulsars observed; $DM < 30 \text{ pc}\cdot\text{cm}^{-3}$
- 40 detected

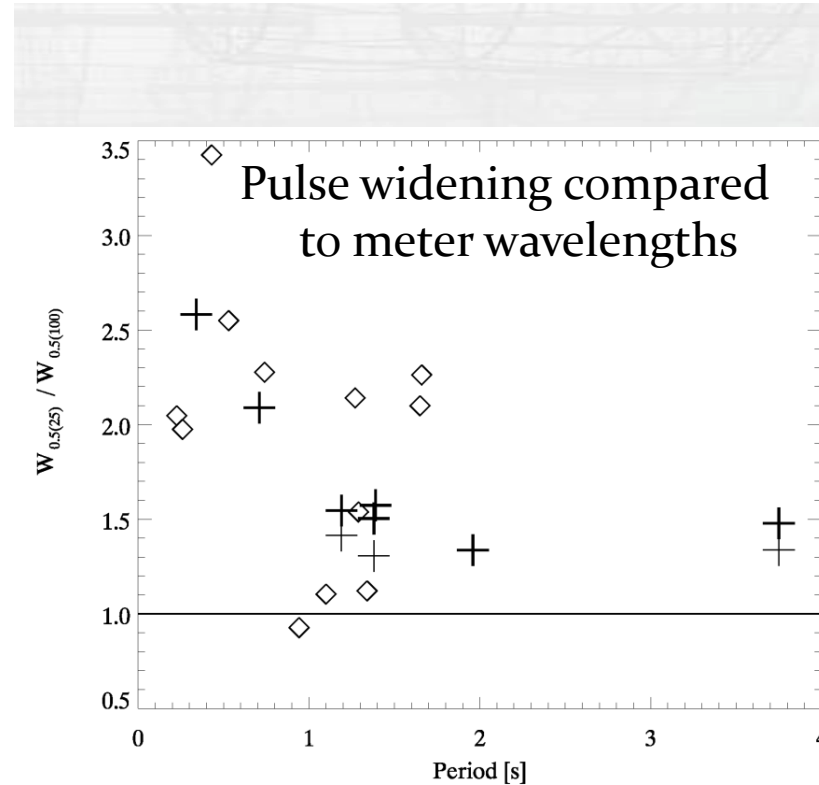
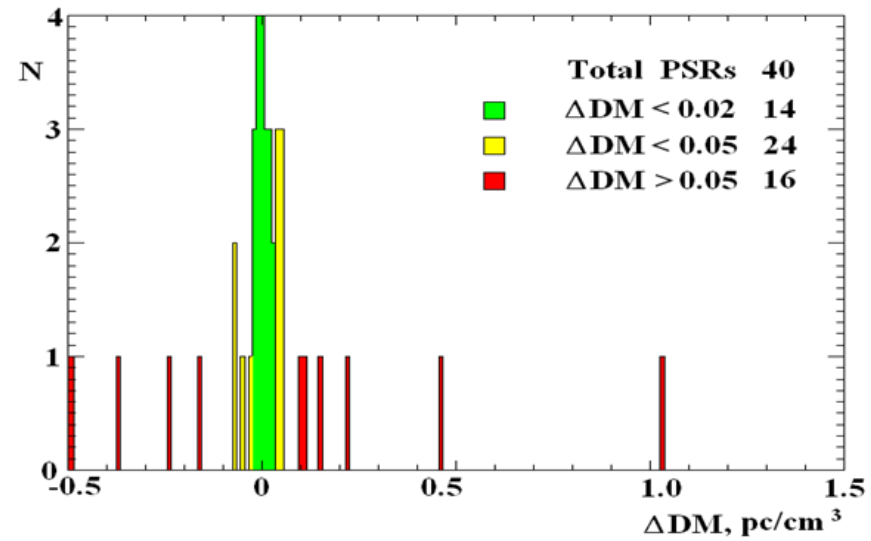
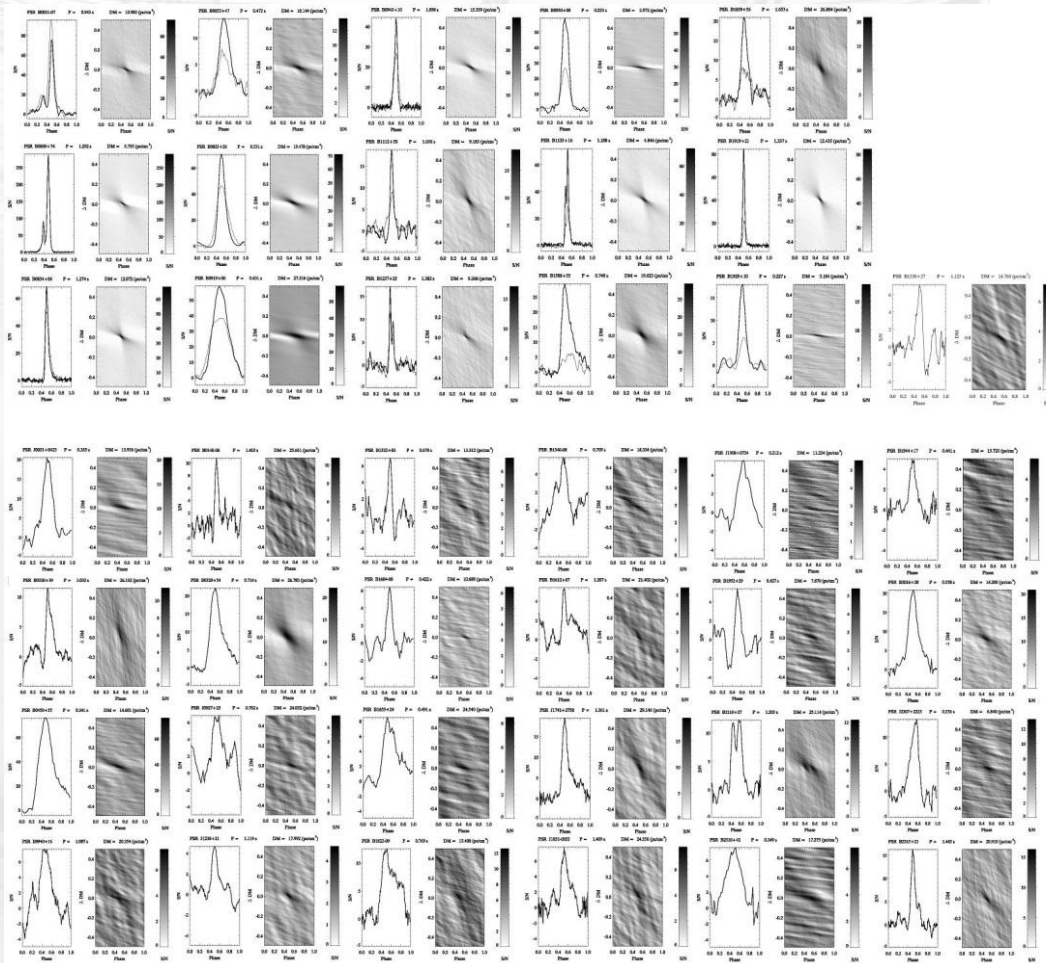
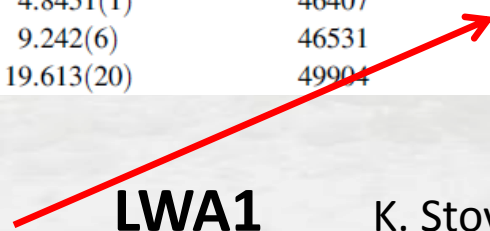


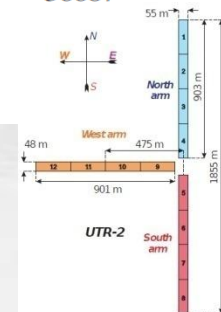
Table 2
Dispersion Measures for 44 Pulsars Detected by LWA1

Pulsar	P (s)	DM_{ATNF} (pc cm^{-3})	$DM_{\text{Epoch}}^{\text{ATNF}}$	DM_{LWA1} (pc cm^{-3})	$DM_{\text{Epoch}}^{\text{LWA1}}$	DM_{UTR2} (pc cm^{-3})	$DM_{\text{Epoch}}^{\text{UTR2}}$
J0030+0451	0.0049	4.333(1)	50984	4.33252(4)	56560
B0031-07	0.9430	11.38(8)	46635	10.922(6)	56843	10.896(4)	55480
J0034-0534	0.0019	13.76517(4)	50690	13.76505(4)	56631
B0138+59	1.2229	34.797(11)	49293	34.926(4)	56563
B0149-16	0.8327	11.922(4)	48227	11.92577(4)	56955
B0301+19	1.3876	15.737(9)	49289	15.68(3)	57035
B0320+39	3.0321	26.01(3)	49290	26.173(2)	56563	26.162(11)	55480
B0329+54	0.7145	26.7641(1)	46473	26.779(1)	56364	25.661(11)	55480
B0355+54	0.1564	57.1420(3)	49616	57.1453(8)	56674
B0450+55	0.3407	14.495(7)	49910	14.5943(9)	56564	14.602(5)	55480
B0525+21	3.7455	50.937(17)	54200	50.93(1)	56565
B0628-28	1.2444	34.468(17)	46603	34.425(1)	56706
B0655+64	0.1957	8.771(5)	48806	8.777(1)	56639
B0809+74	1.2922	5.733(1)	49162	5.771(2)	56285	5.755(3)	55480
B0818-13	1.2381	40.938(3)	48904	40.981(2)	56568
B0823+26	0.5307	19.454(4)	46450	19.4789(2)	56665	19.484(6)	55480
B0834+06	1.2738	12.889(6)	48721	12.8640(4)	56864	12.872(4)	55480
B0906-17	0.4016	15.888(3)	48737	15.879(2)	56980
B0919+06	0.4306	27.271(6)	55140	27.2986(5)	56285	27.316(6)	55480
B0943+10	1.0977	15.4(5)	48483	15.334(1)	56365	15.339(4)	55480
B0950+08	0.2531	2.958(3)	46375	2.96927(8)	56285	2.972(2)	55480
B1112+50	1.6564	9.195(8)	49334	9.1830(4)	56687	9.185(4)	55480
B1133+16	1.1879	4.8451(1)	46407	4.8480(2)			
		9.242(6)	46531	9.2575(3)			
		19.613(20)	49904	19.6191(3)			

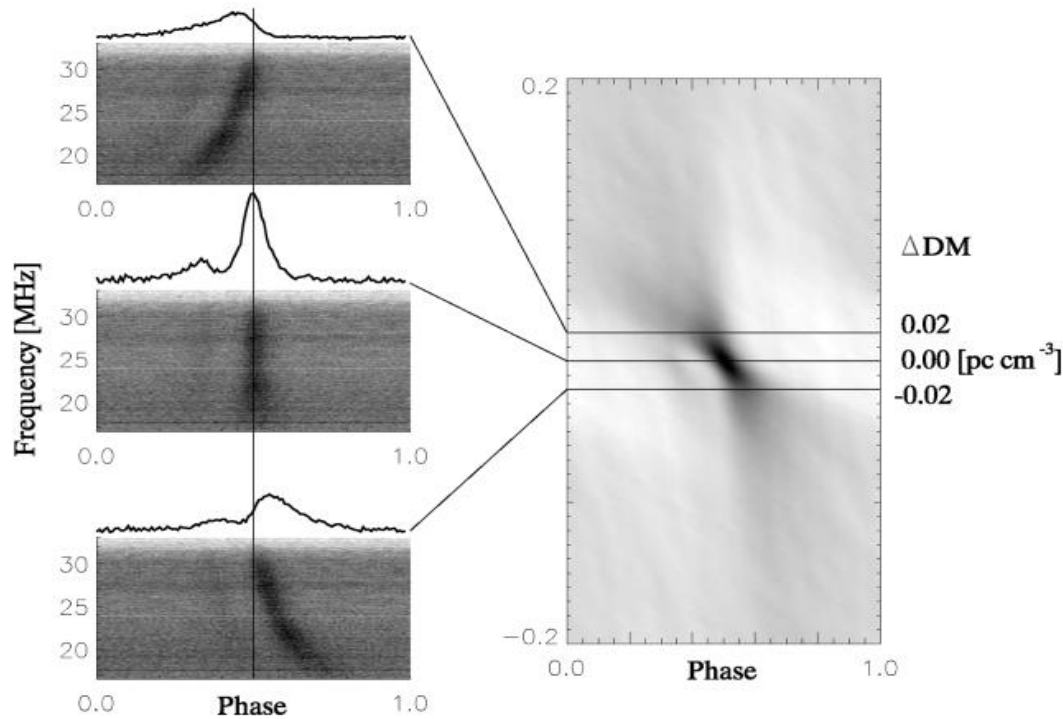


LWA1

K. Stovall et al. 2015



Characteristic view of the broadband signal at the “Dispersion measure - Time” plane



Zakharenko et al., MNRAS, 2013

The slope of the region of maximum intensity is induced by the fact that the compensation of dispersion delay is related to the upper frequency of the range. ‘Undercompensation’ ($\Delta DM < 0$) shifts the average profile to a later phase of the pulsar rotation period, while ‘overcompensation’ ($\Delta DM > 0$) shifts it to an earlier phase (left panels).

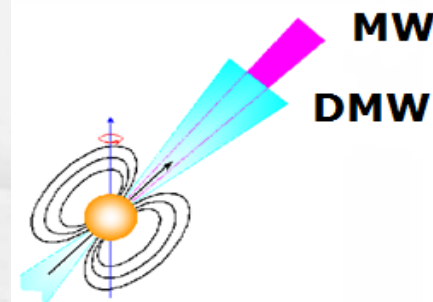
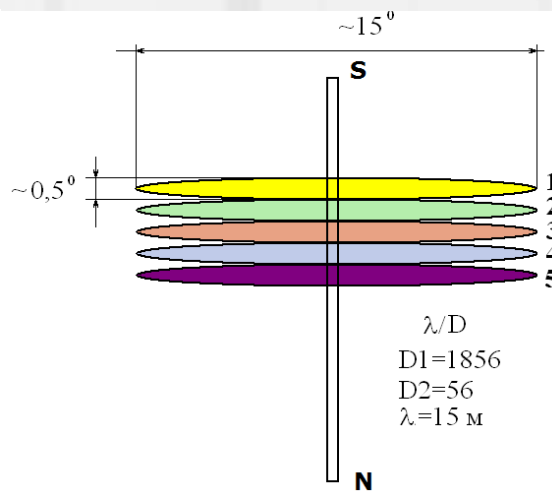
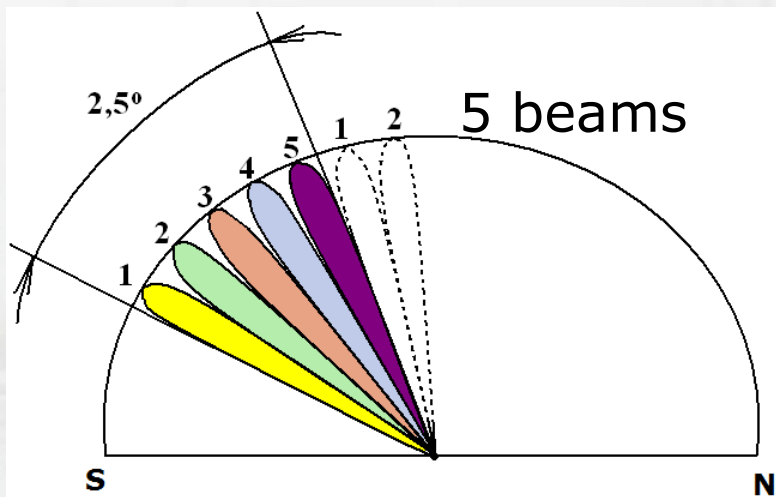
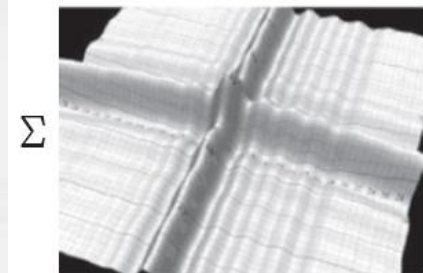
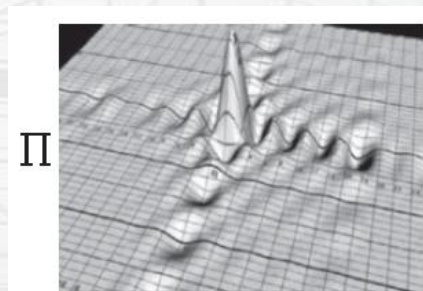
«Such a survey – “blind” and fullsky – is both useful,
required and achievable!»

Decameter pulsar/transient survey of northern sky.
Drift-scan method, UTR-2

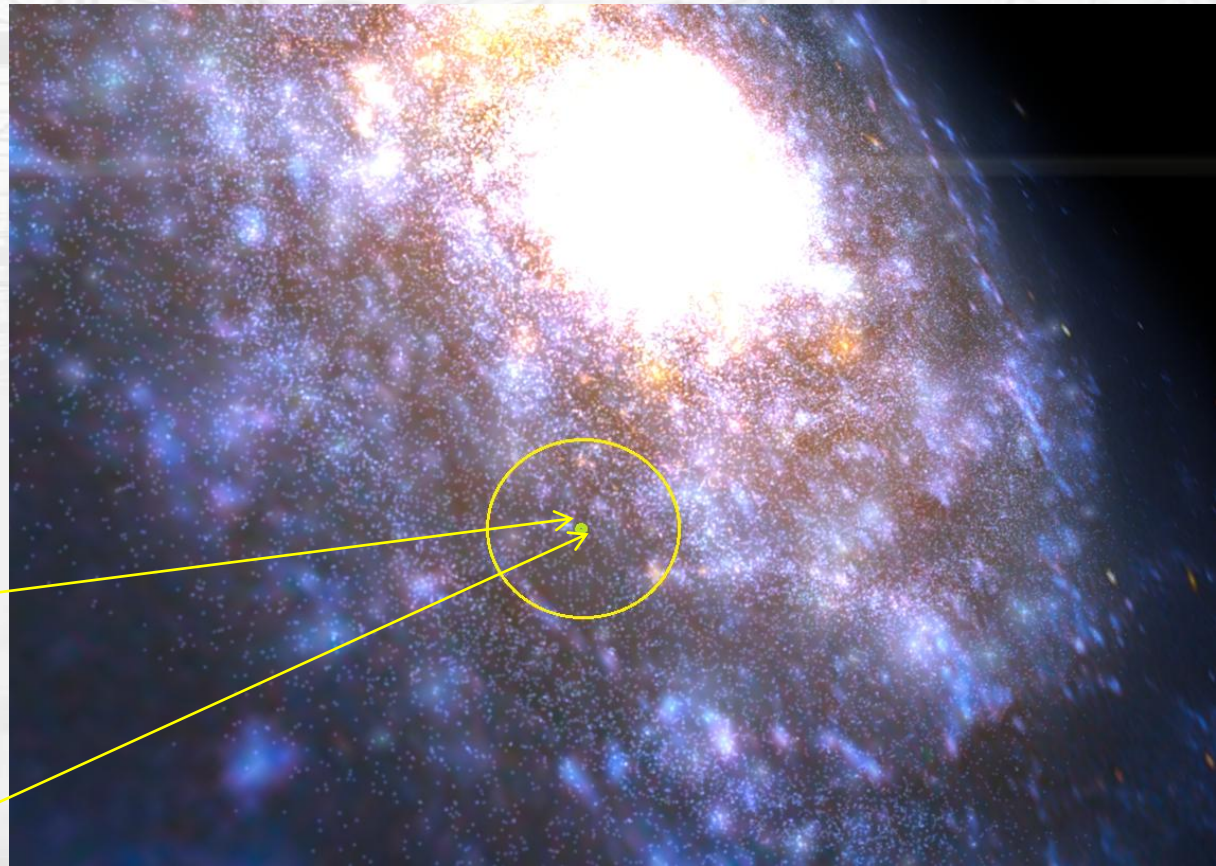
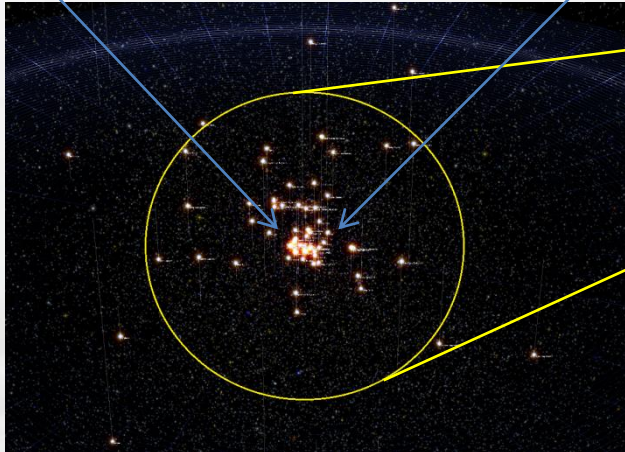
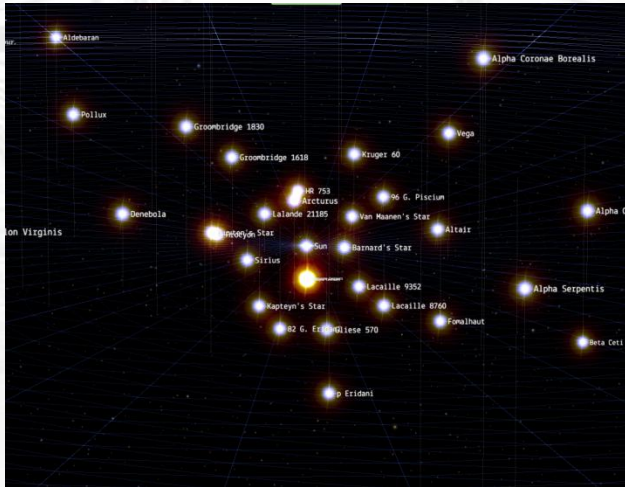
DM: 0...30
pc·cm⁻³,

Δt=8 msec,

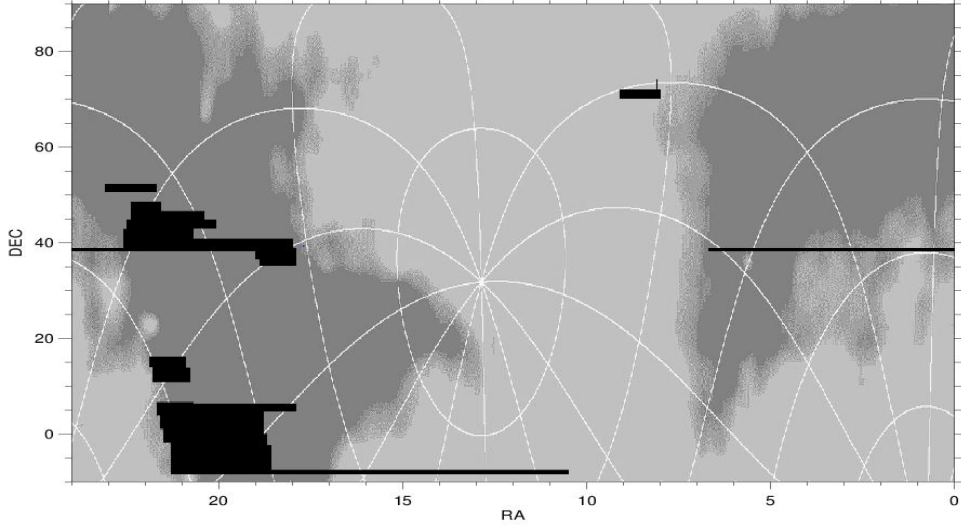
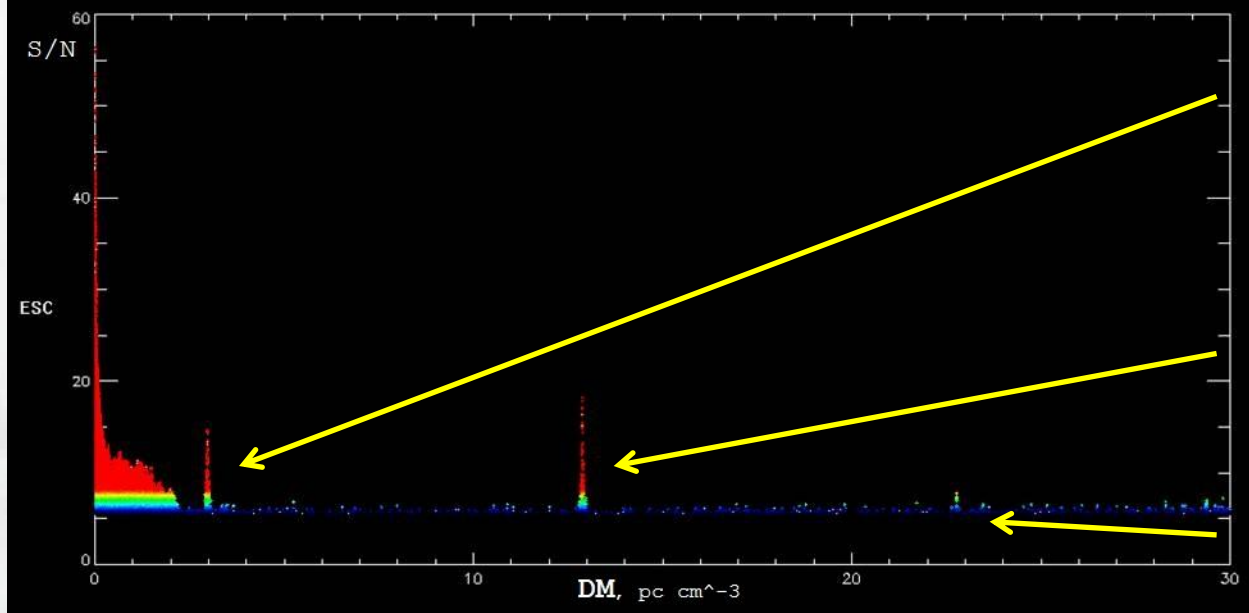
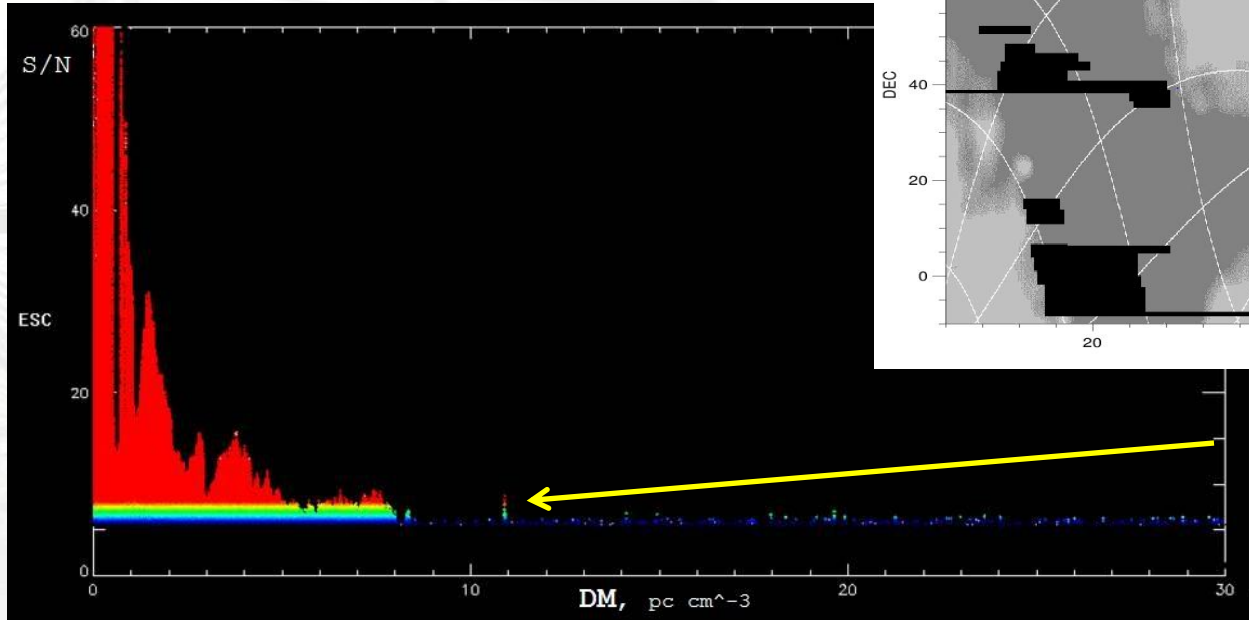
dec.: -10...90
deg.



Nearest galactic surroundings



Automatic events search: "SNR vs DM" plane



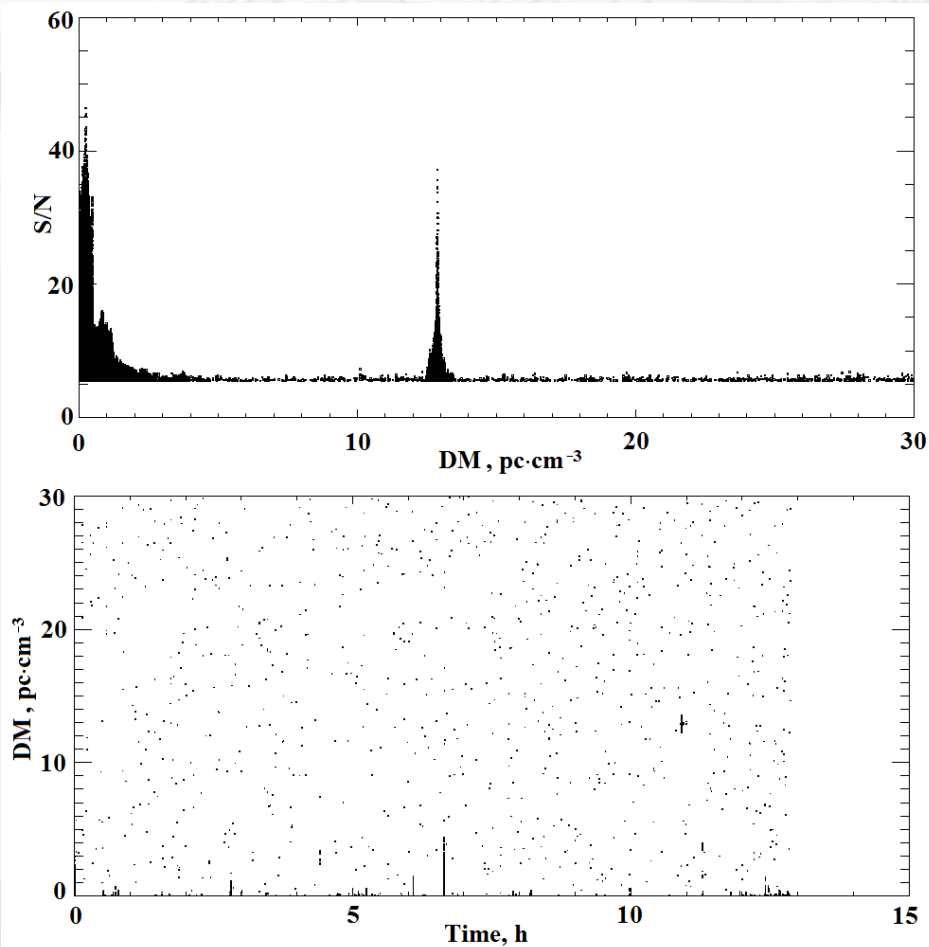
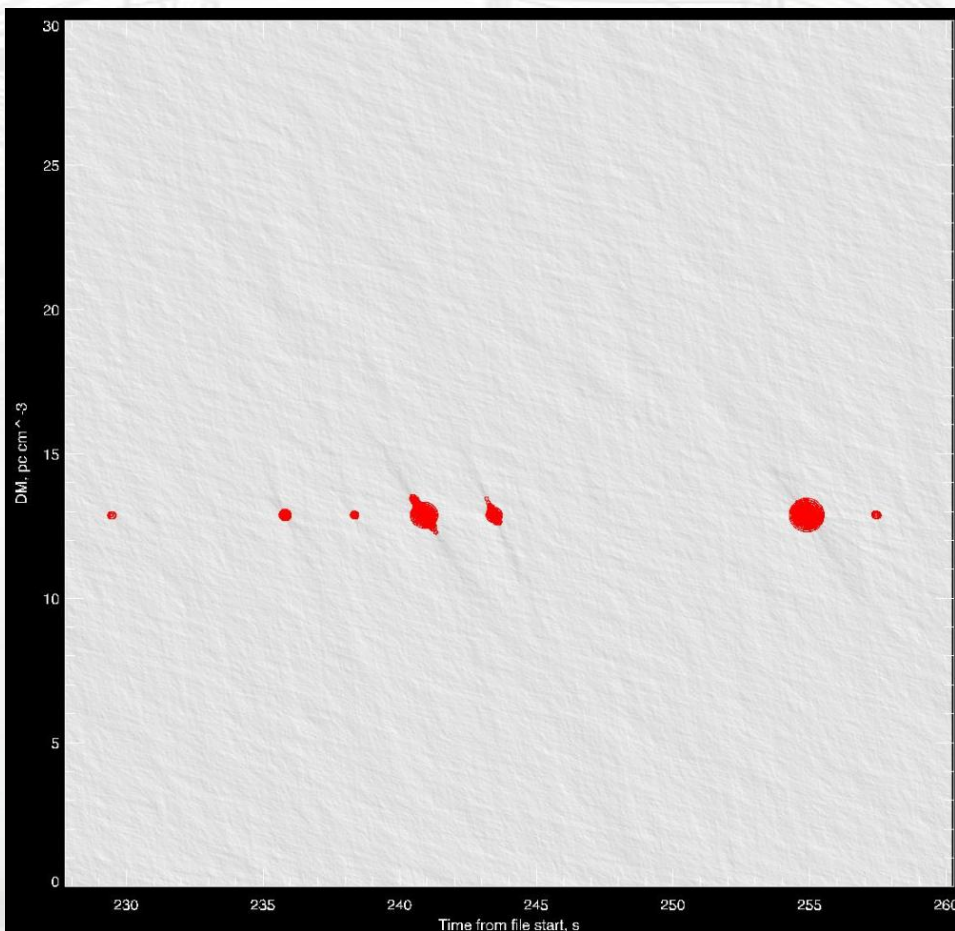
PSR B0031-07

PSR B0950+08

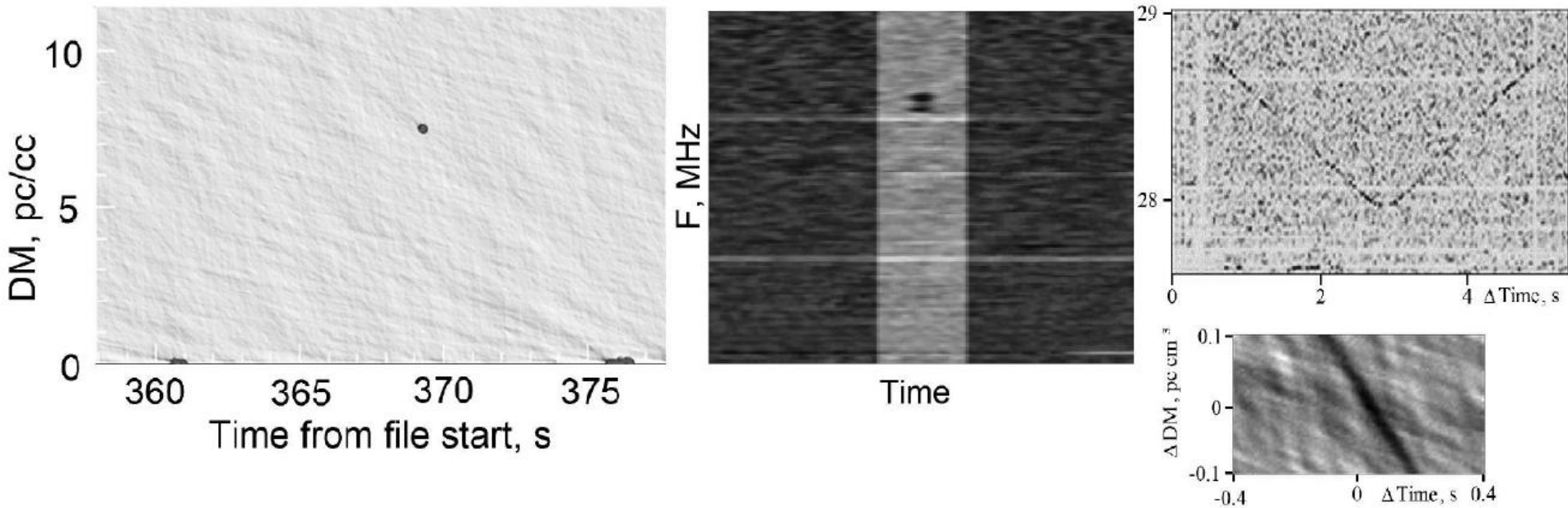
PSR B0834+06

?

Code V717, receiver E
@ DM=12.8800 with SNR 37.1787 at 10h55m 0.074s. File:76 frame:8



Example of RFI found by means of "short pipeline"



[I. P. Kravtsov, V. V. Zakharenko et al., AASP, 2016](#)

Identifying the source of perytons at the Parkes radio telescope

E. Petroff^{1,2,3*}, E. F. Keane^{1,4,3}, E. D. Barr^{1,3}, J. E. Reynolds², J. Sarkissian², P. G. Edwards², J. Stevens², C. Brem², A. Jameson¹, S. Burke-Spolaor⁵, S. Johnston², N. D. R. Bhat^{6,3}, P. Chandra⁷, S. Kudale⁷, S. Bhandari^{1,3}

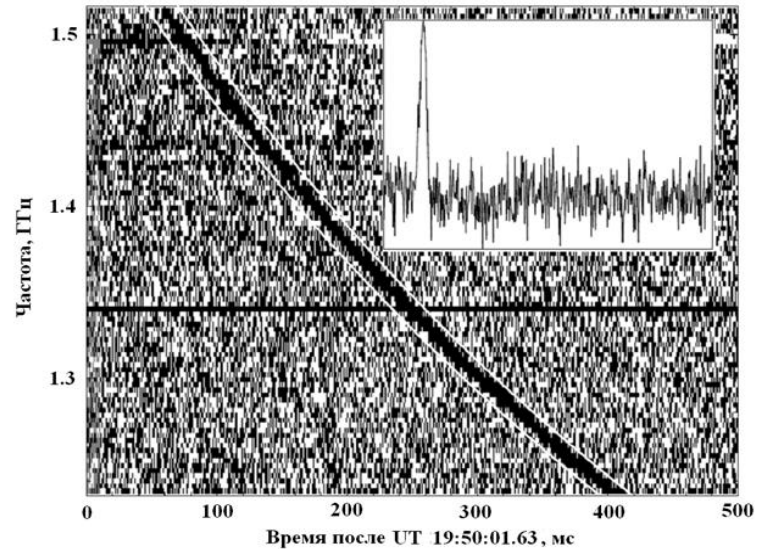
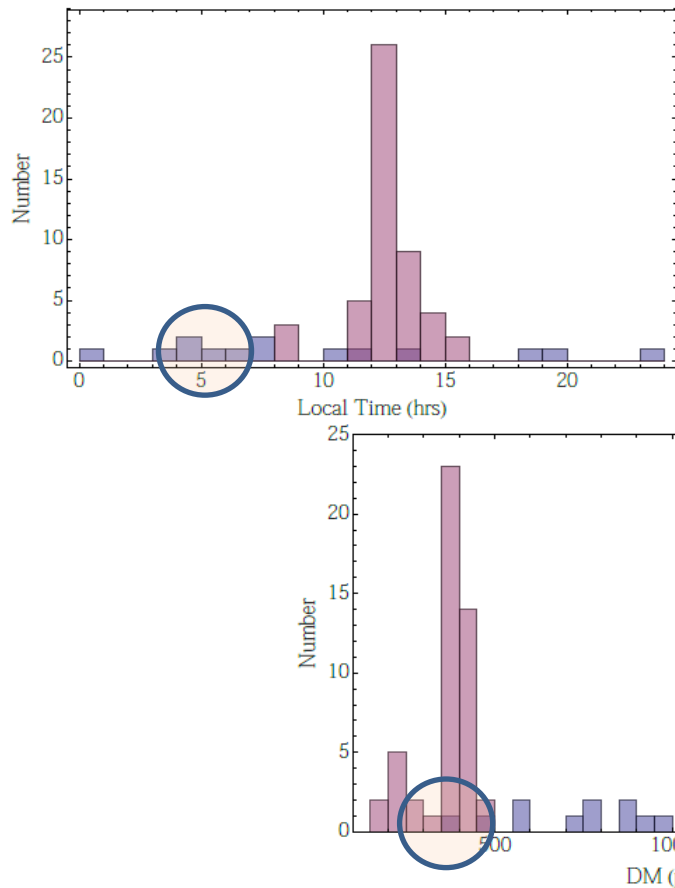
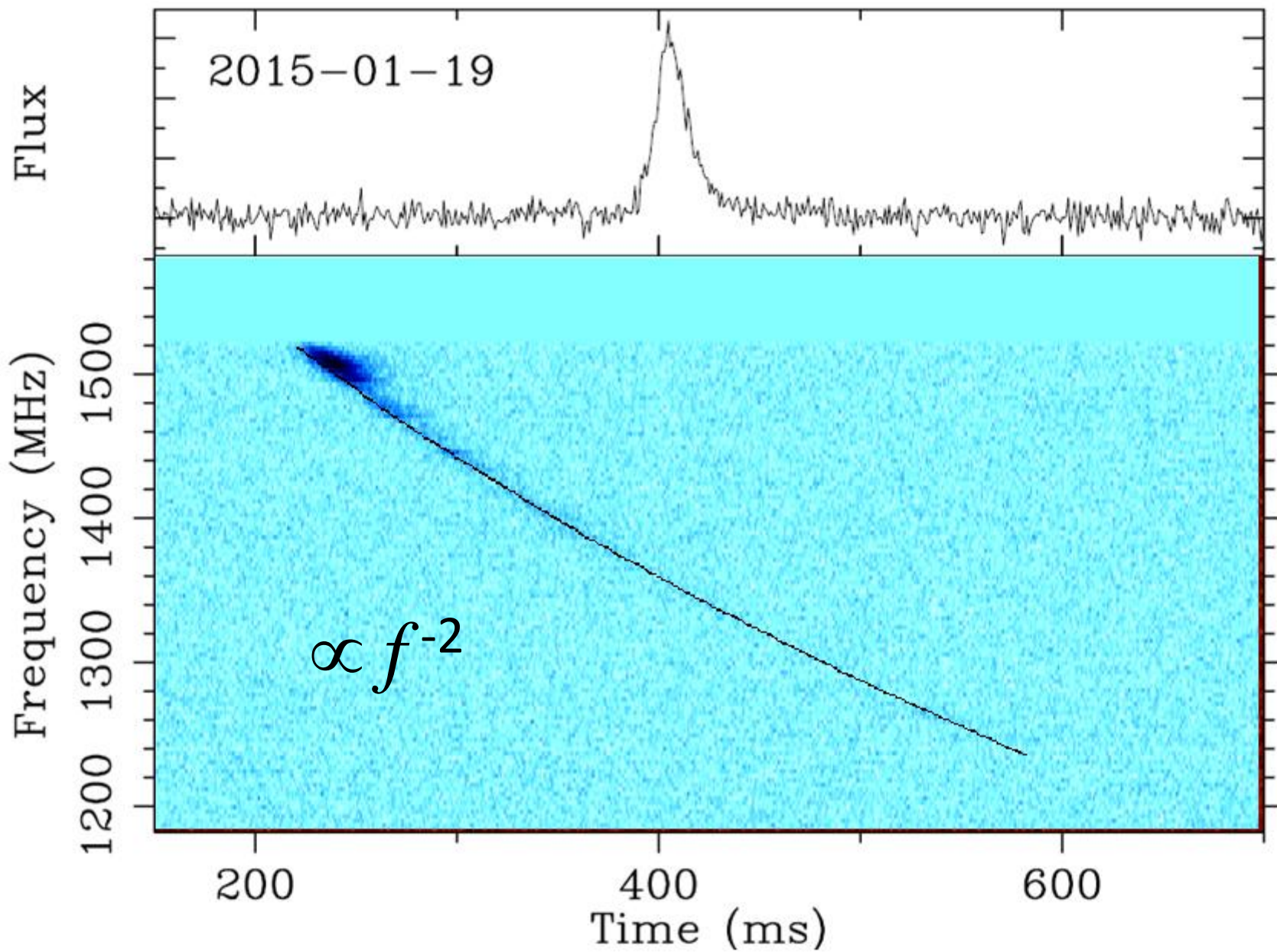
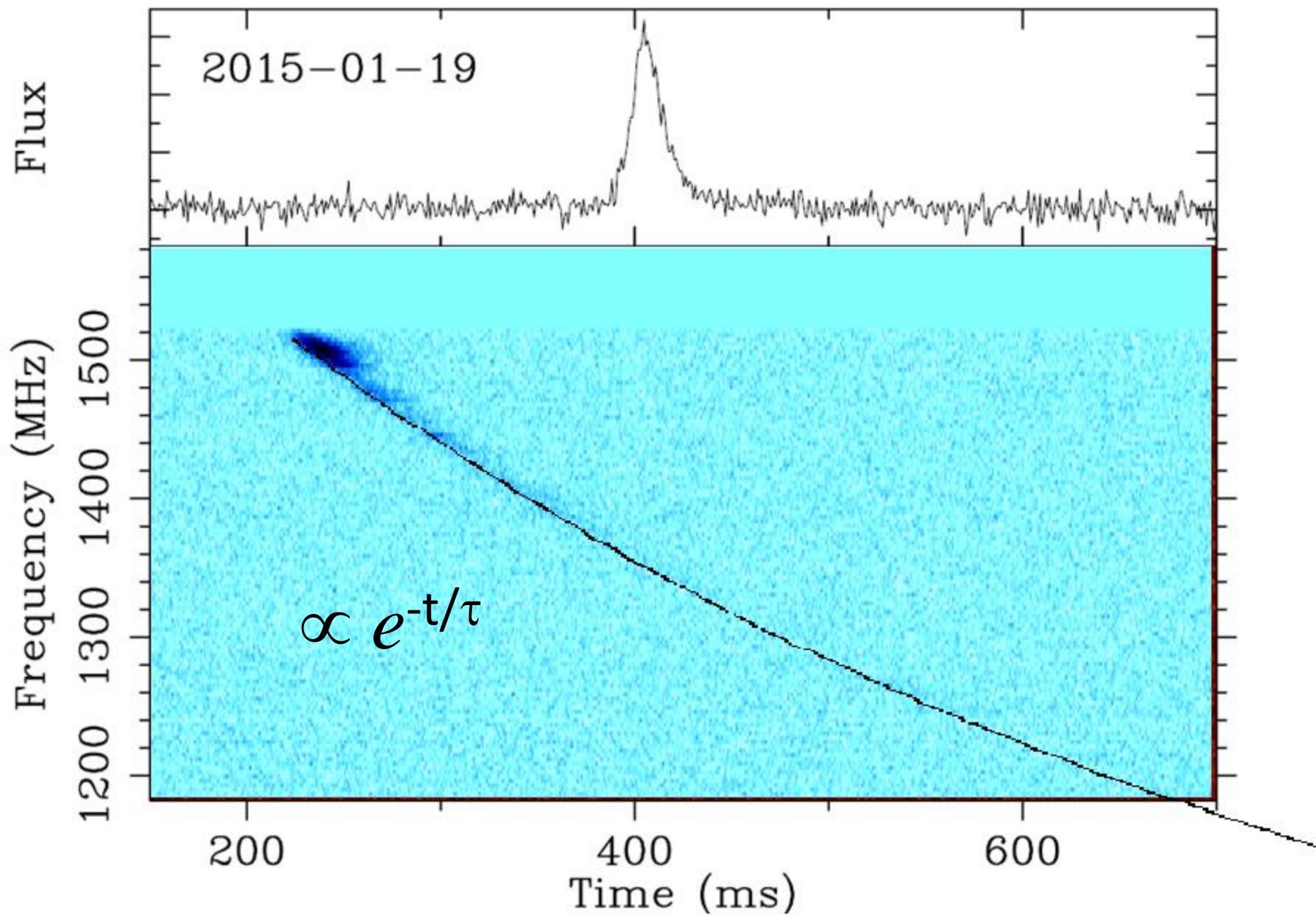


Рис.1.3. “Lorimer burst” (FRB 010724) из работы [180] Представлены динамические спектры и проинтегрированный профиль всплеска 24 июля 2001 г. DM равна 375 ± 1 пк см⁻³. Разделив данные на четыре субполосы были получены и характеристики времени рассеяния. Его описывает степенной закон со спектральным индексом -4 ± 1 .

even a well-known Lorimer burst was suspected

Figure 7. The FRB (blue) and peryton (red) distributions as a function of the local time with Australian Eastern Daylight Savings Time accounted for (top left), time in Australian Eastern Standard Time (top right) and as a function of the entire range searched (bottom). Clearly the FRB distribution is uniform throughout the day, whereas the peryton signals peak strongly during office hours (particularly around lunch time). A random distribution would look approximately flat, with a slight dip during office hours where occasional maintenance is carried out. The bi-modal peryton distribution with peaks at ~ 200 and ~ 400 cm⁻³ pc is evident.





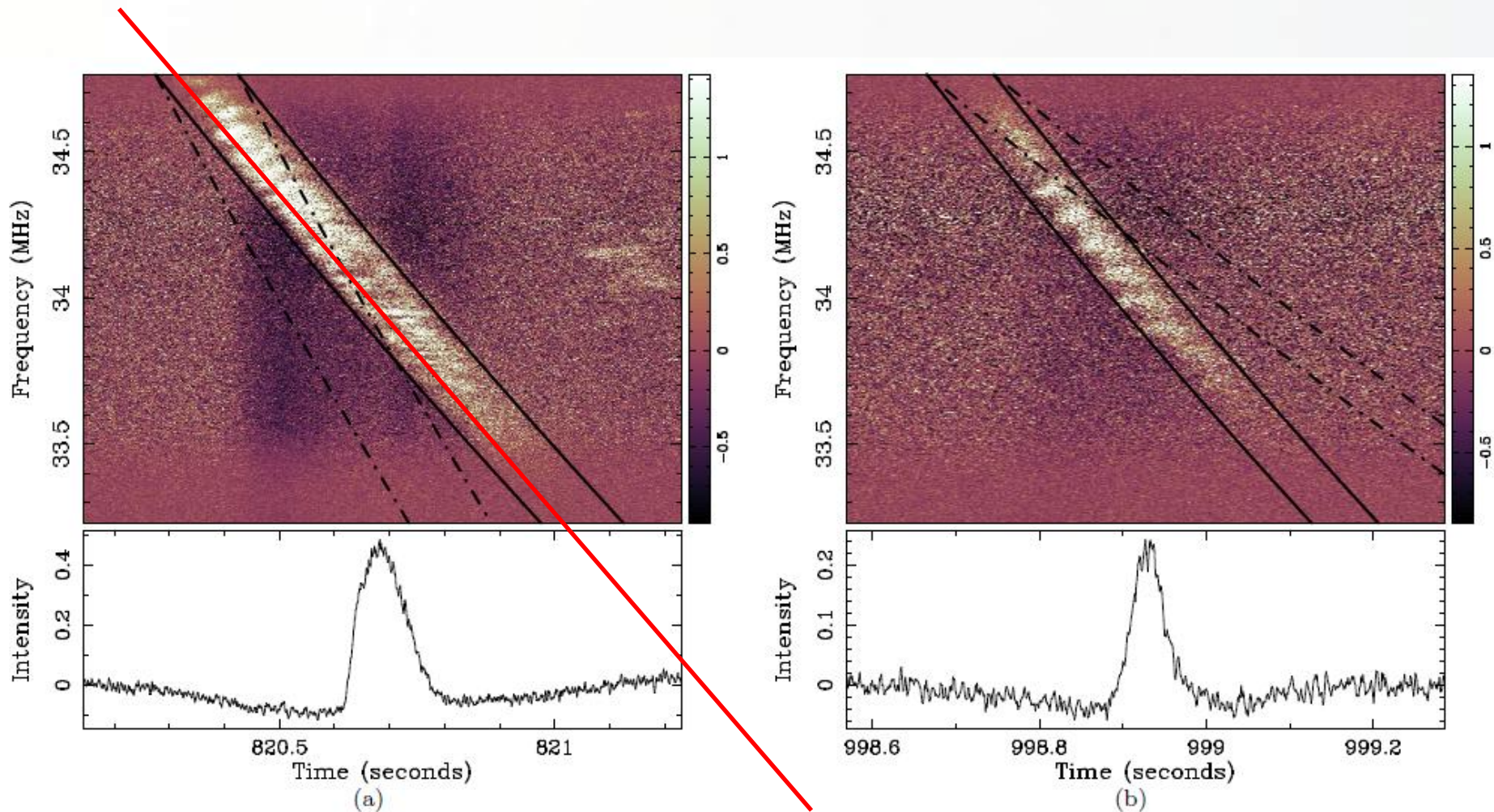
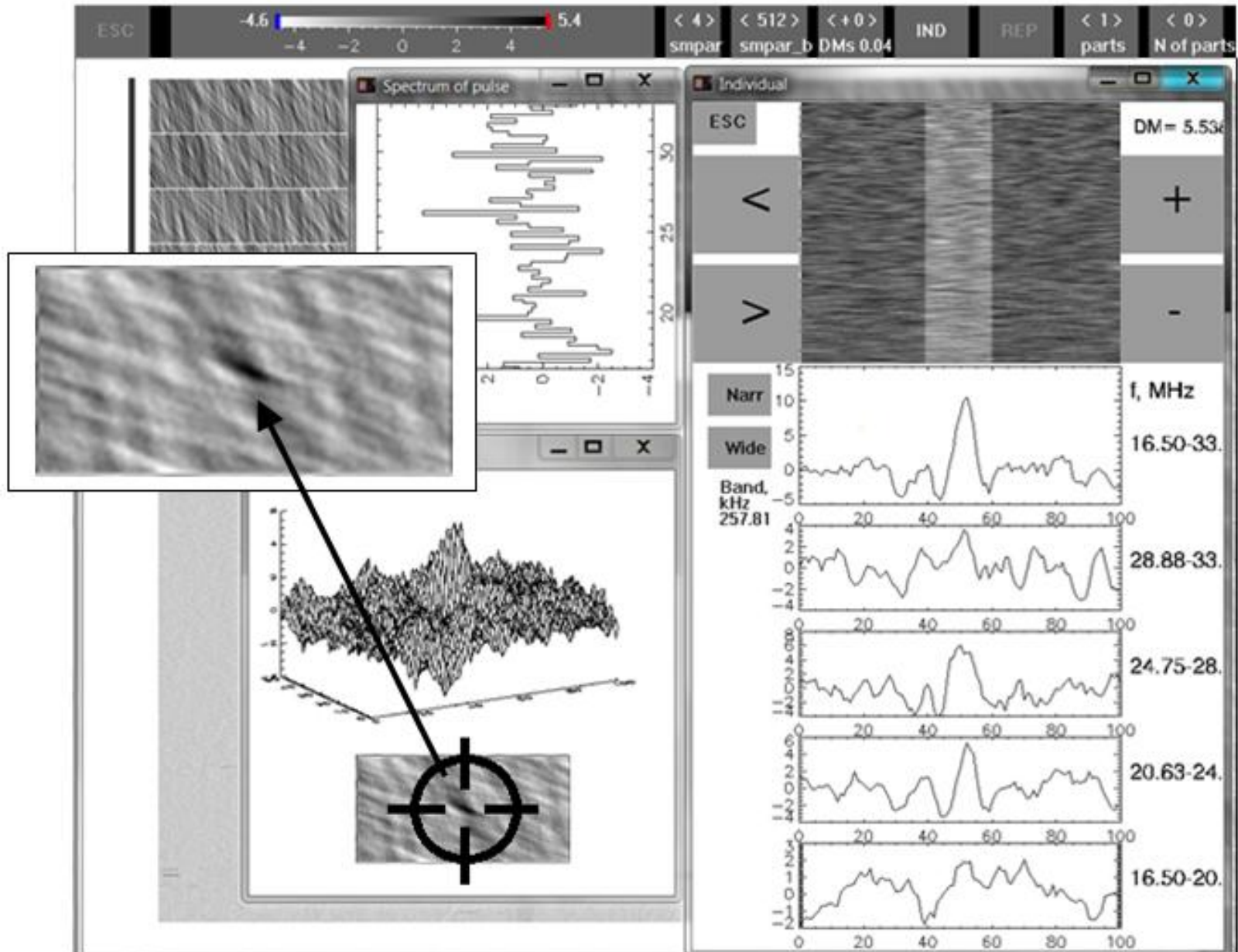


FIG. 1.— Two bright radio bursts discovered in session A: In each of the subfigures (a) and (b), the upper panel shows a part of the dynamic spectrum centered at the position of the burst. The pairs of continuous slanted lines that bound the pulse, show the expected quadratic behavior for the cold-plasma dispersion relation, corresponding to the respective best-estimated DMs — 2.16 pc cm^{-3} and 1.42 pc cm^{-3} for the bursts in subfigures (a) and (b), respectively. To demonstrate the difference in the two DM values, the dash-dot-dashed lines in subfigure (a) shows the dispersion relation corresponding to the DM of the burst in (b), and vice-versa. The lower panels show the total intensity as a function of time measured from the start of the observation, after dispersive delays are corrected using the corresponding best-estimated DMs (for a reference frequency of 34 MHz). The intensity in both the panels is in units of system temperature.

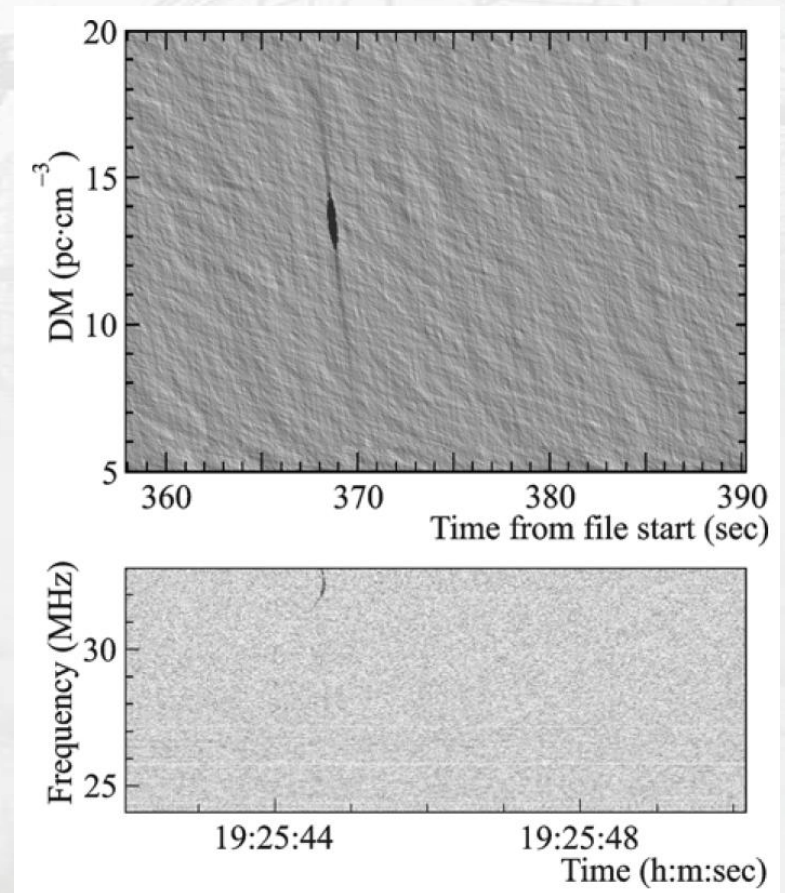
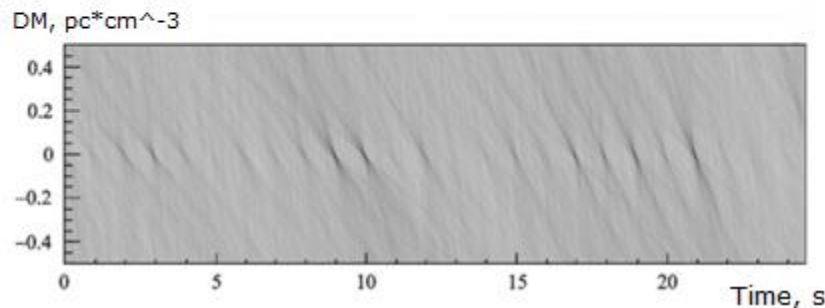
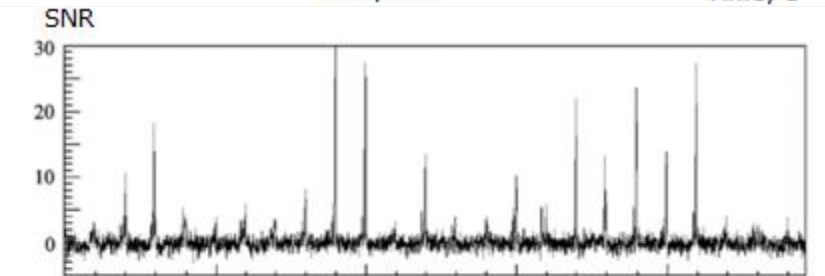
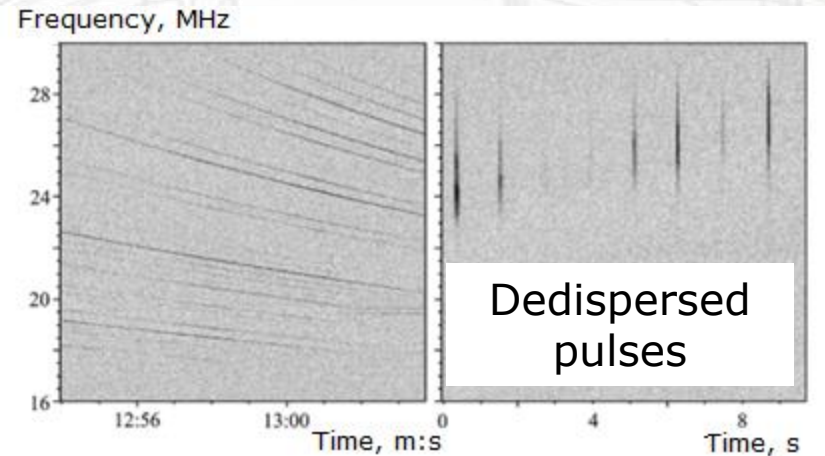
Transient signal "candidate". Multi-parametric search



First stage: RFI mitigation

Second stage: dedispersion in range $0 \dots 30 \text{ pc} \cdot \text{cm}^{-3}$ with a step 0.01.

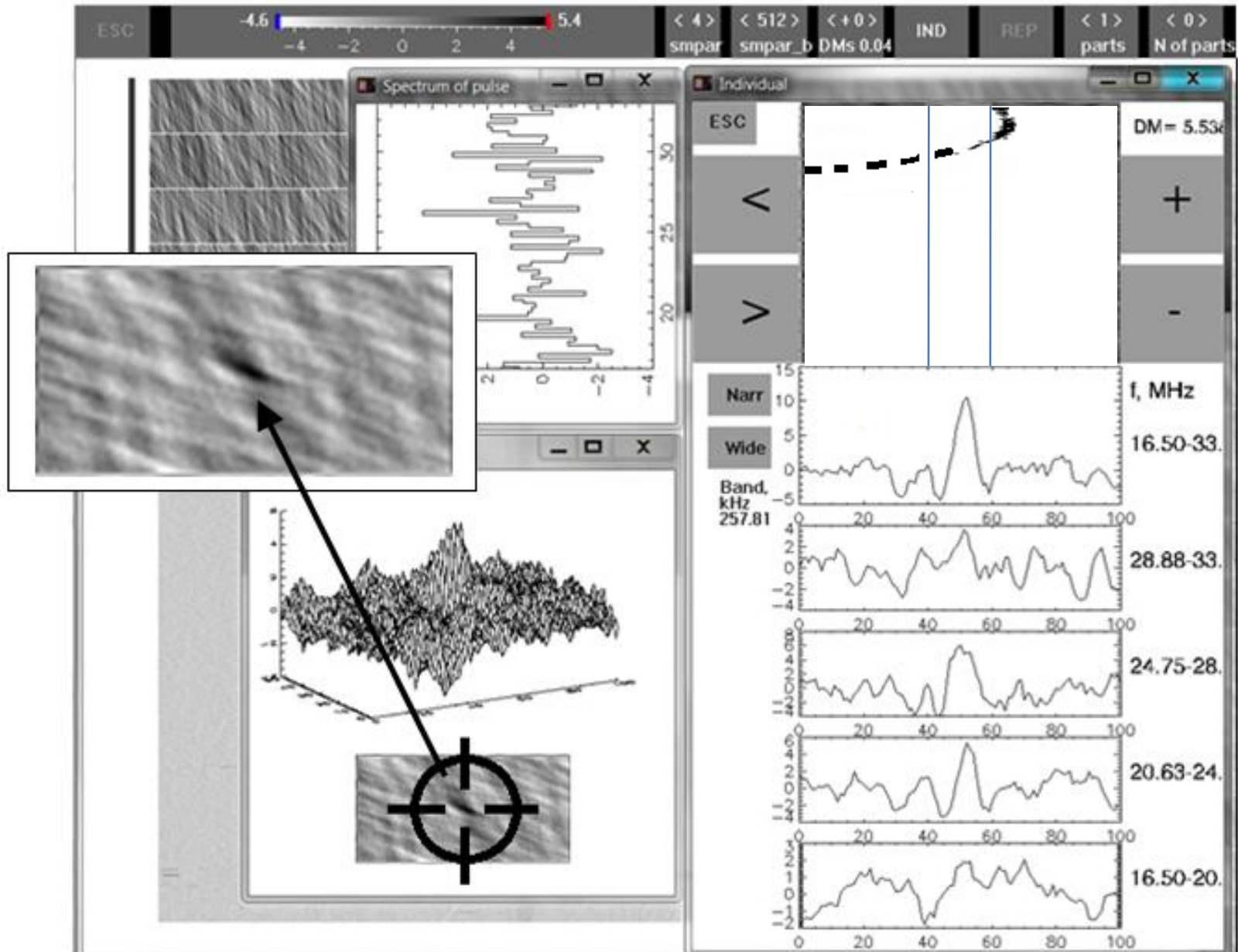
Third stage: candidate selection (step up to $0.002 \text{ pc} \cdot \text{cm}^{-3}$). It allows to distinguish very reliably between broadband cosmic signals with dispersion law $\propto f^{-2}$ and signals with different time-frequency dependences.



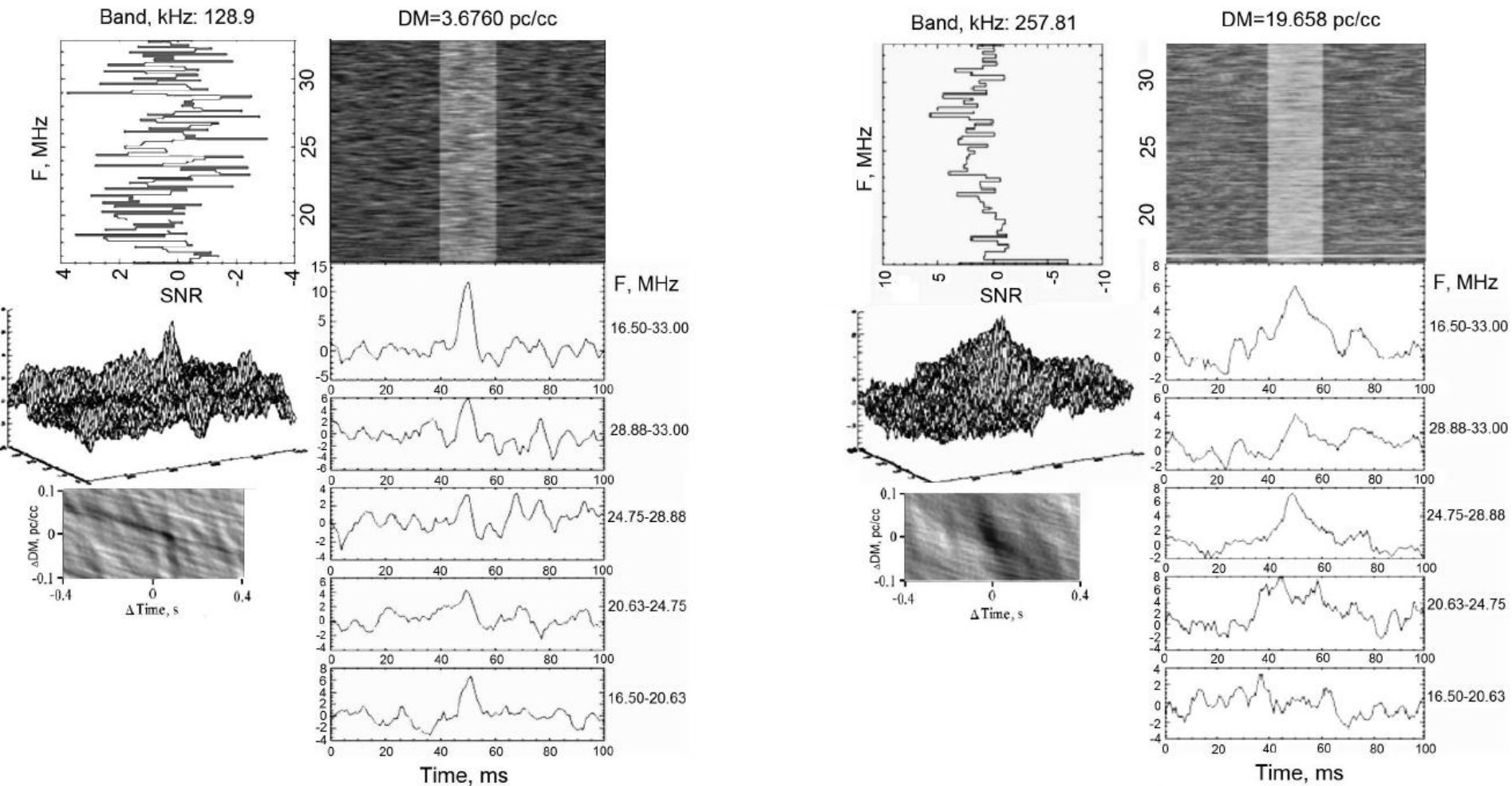
RFI with linear frequency modulation and it's representation on «DM vs time» plane

Pulses of PSRB0809+74 in the range of $\text{DM} \pm 0.5 \text{ pc} \cdot \text{cm}^{-3}$

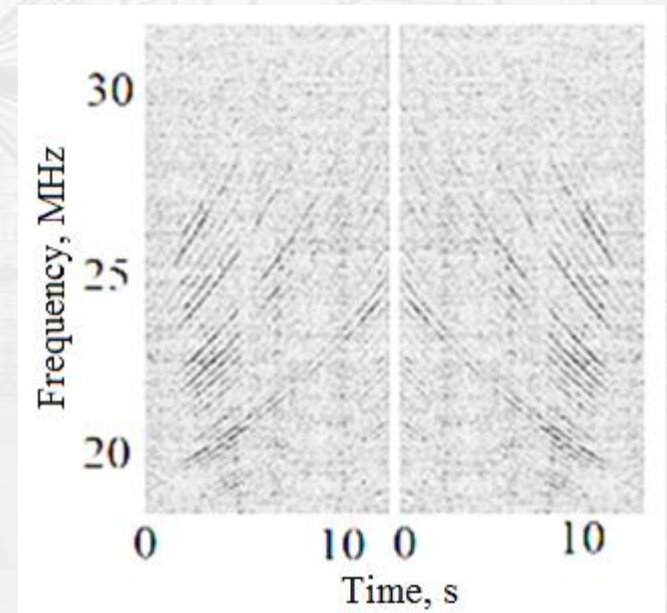
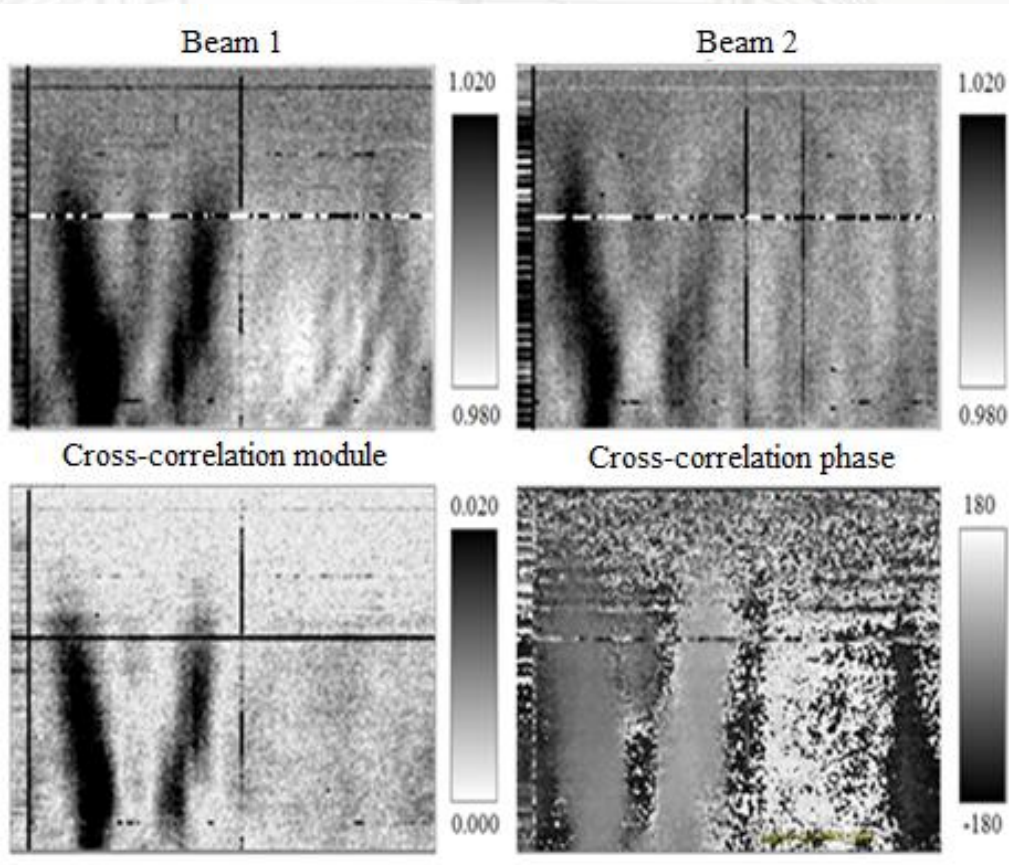
to distinguish reliably $\propto f^{-p}$ where p in [1.98...2.02]



Example of a transient signal from an unknown source (left) and weak pulse of PSRB1508+55



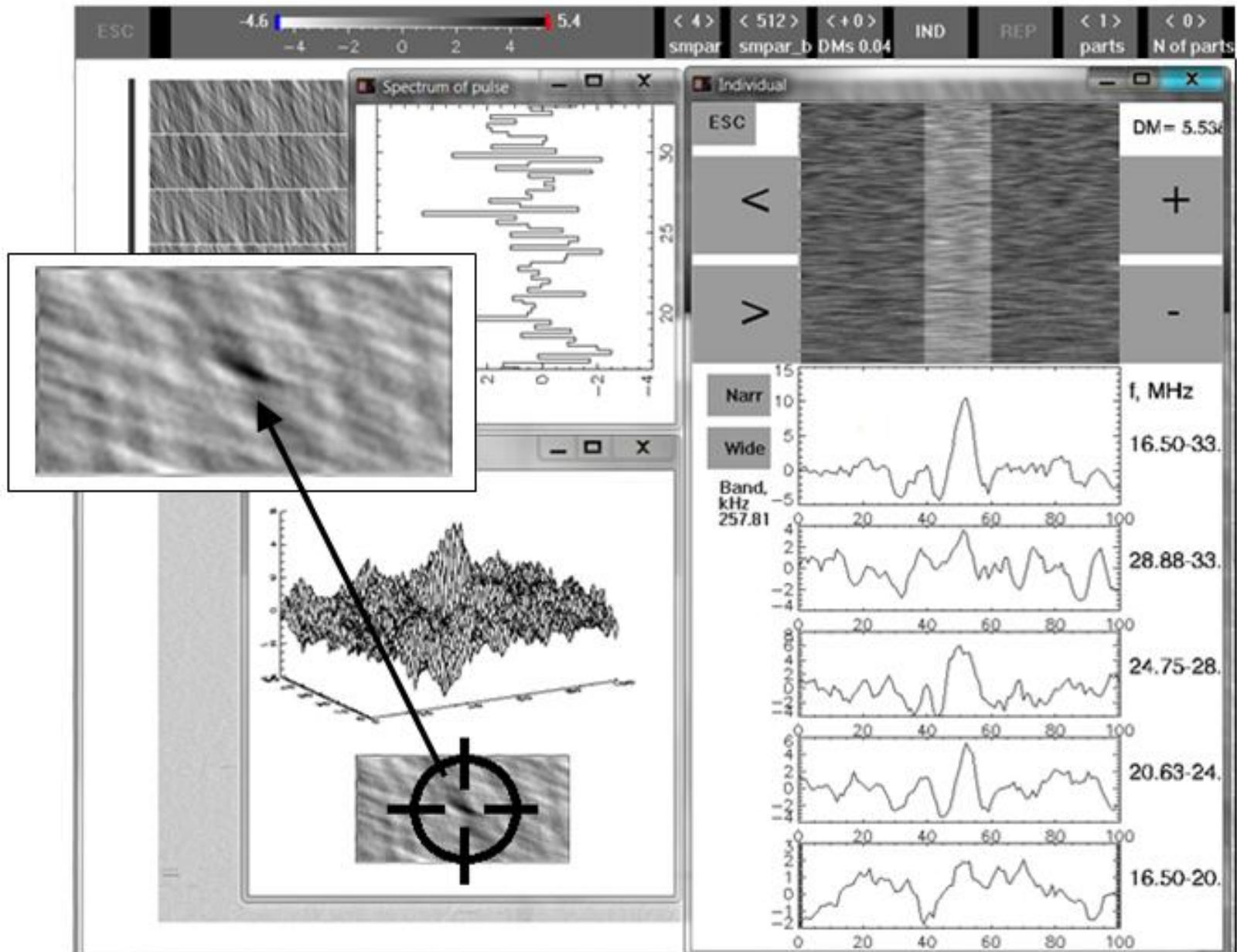
Ionospheric scintillations with a different sign of the time-frequency delay. **“Inverse” DM test**



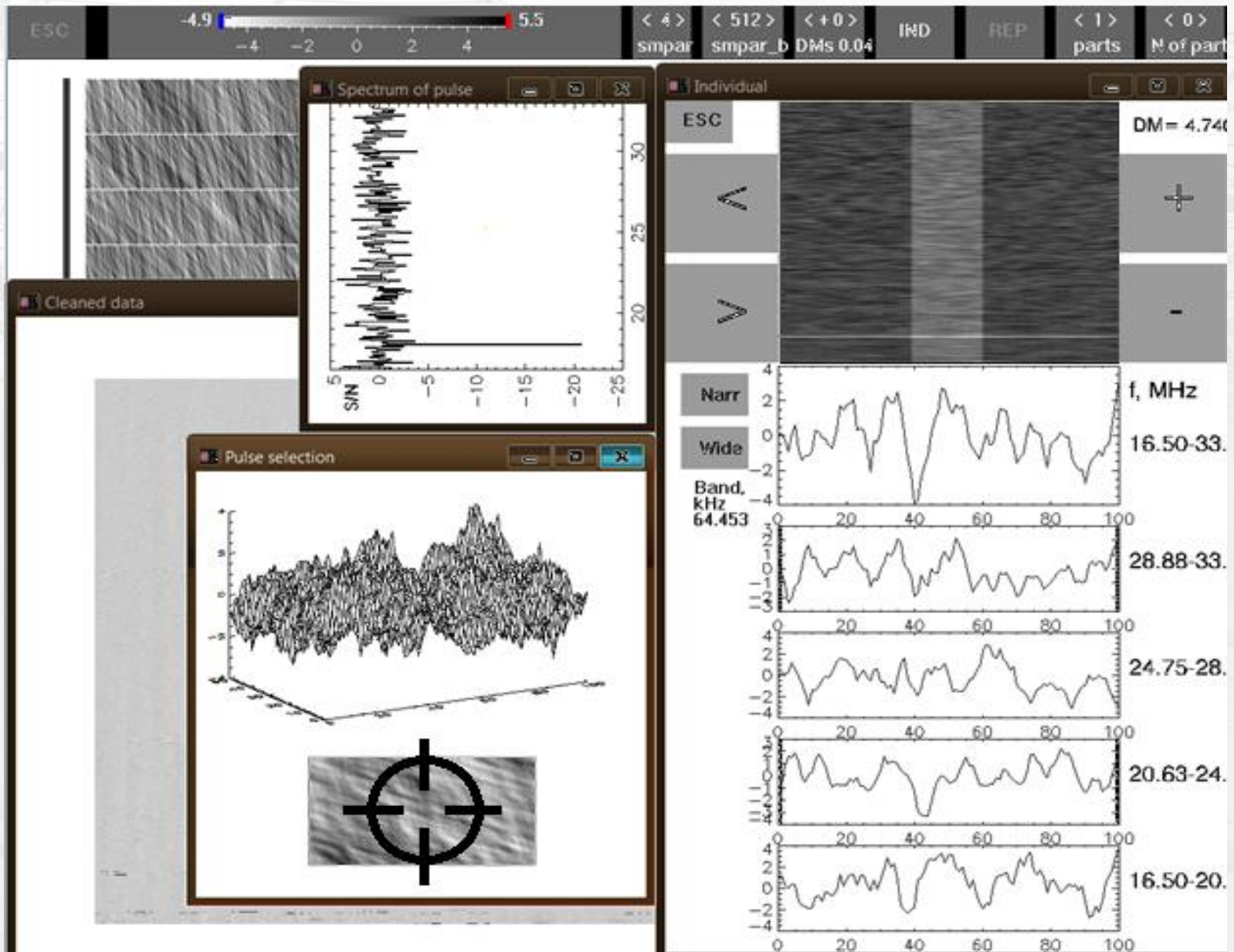
Signals of PSR B0809+74, inverted in time with the “inverse” dispersion dependence (left) and the same output data.

Examples of wide band scintillations with a different time-frequency slope

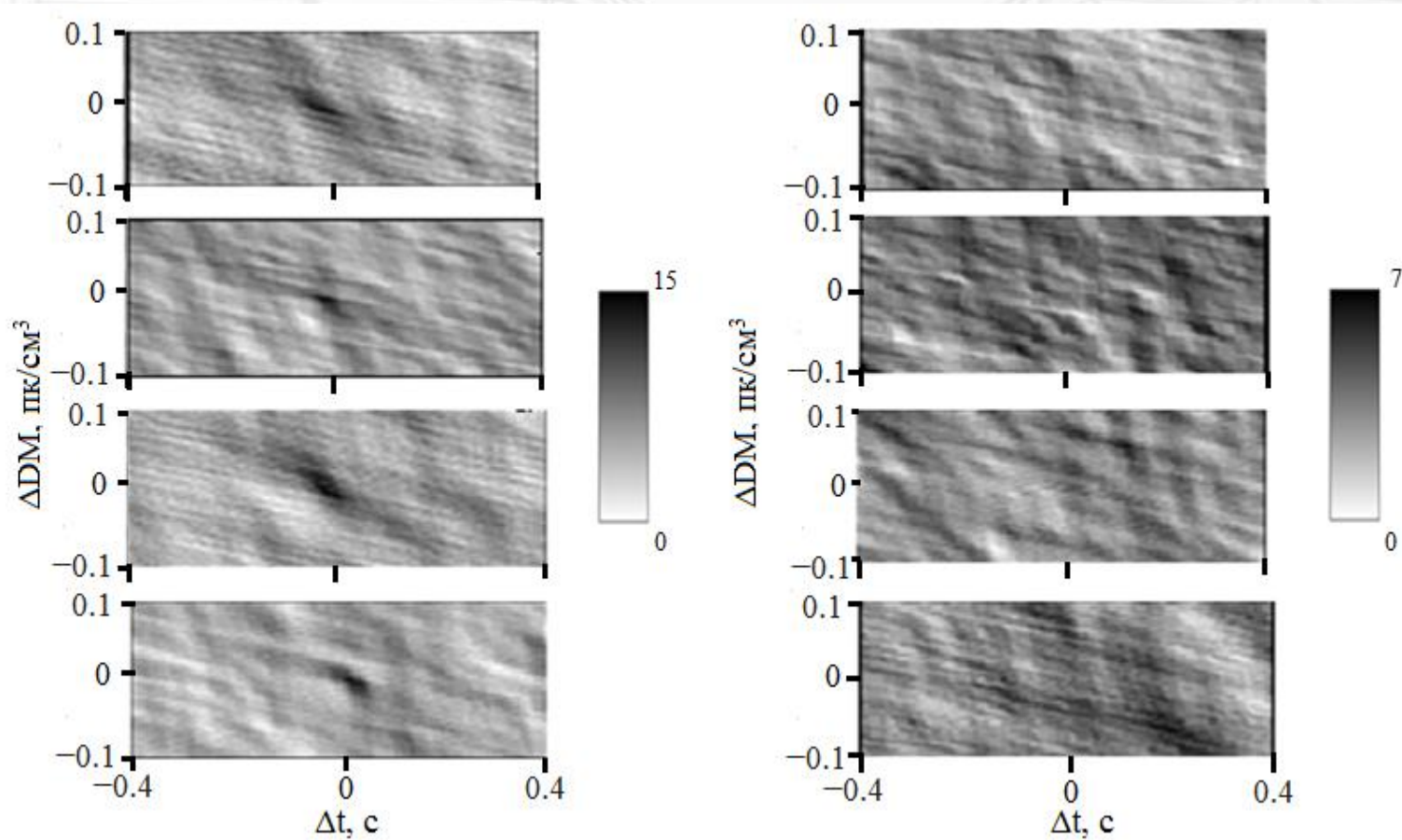
Transient signal (candidate) (“direct” DM)



Interference (“inverse” DM)



Comparison of the signals with a “direct” (left) and “inverse” DM

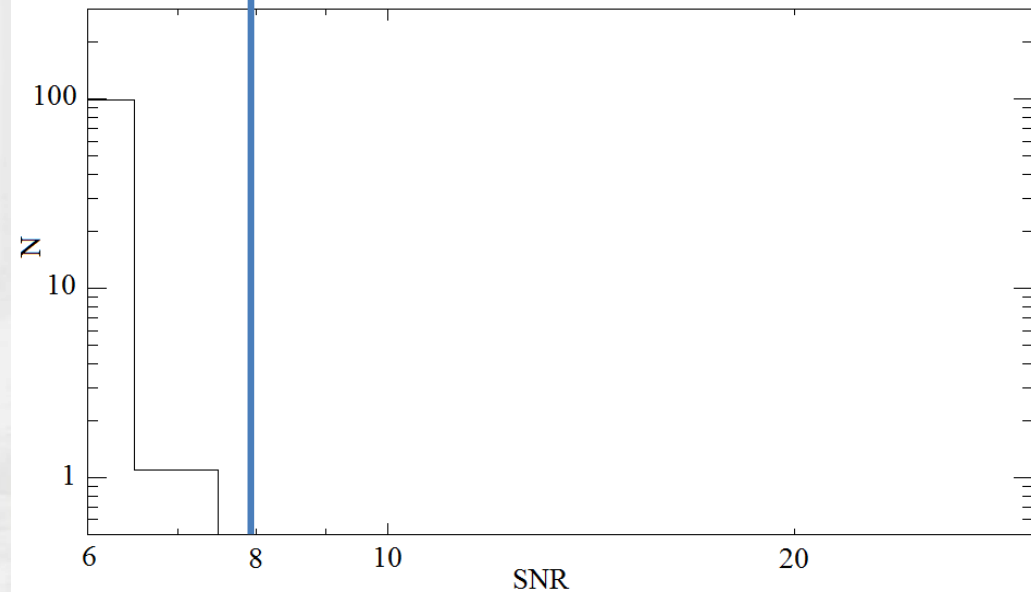
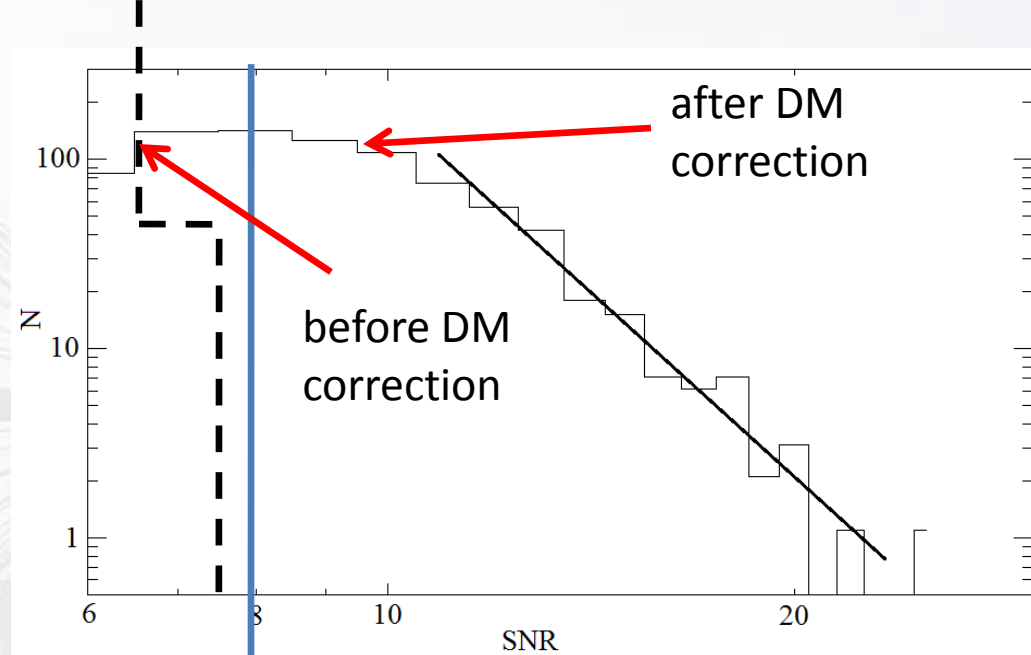
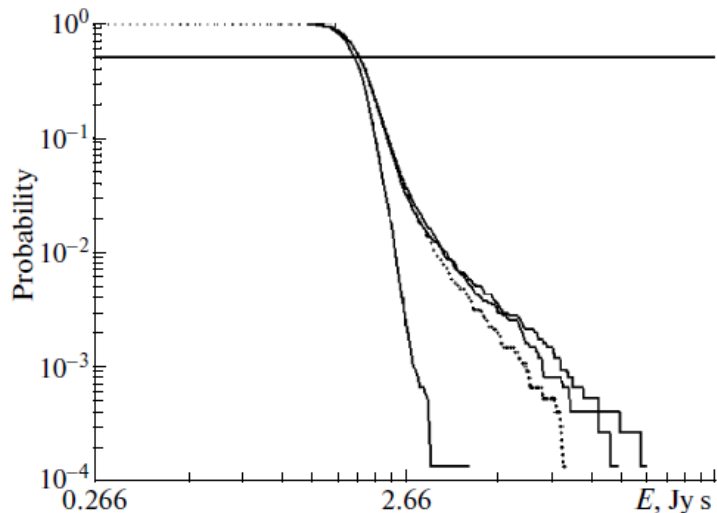


2-dimensional “DM - Time” dependences ($\pm 0.1 \text{ pc/cm}^3$ in DM and $\pm 400 \text{ ms}$ in time). Left panel shows candidate signals found in the Survey. Right one - “DM - Time” dependencies for the signals with the “inverse” (dispersion delay is proportional to f^{-2}). Candidate signals have sloping high intensity oval in the center of 2-dimensional dependence. Signals found in the inverted data don’t have such a wide maxima.

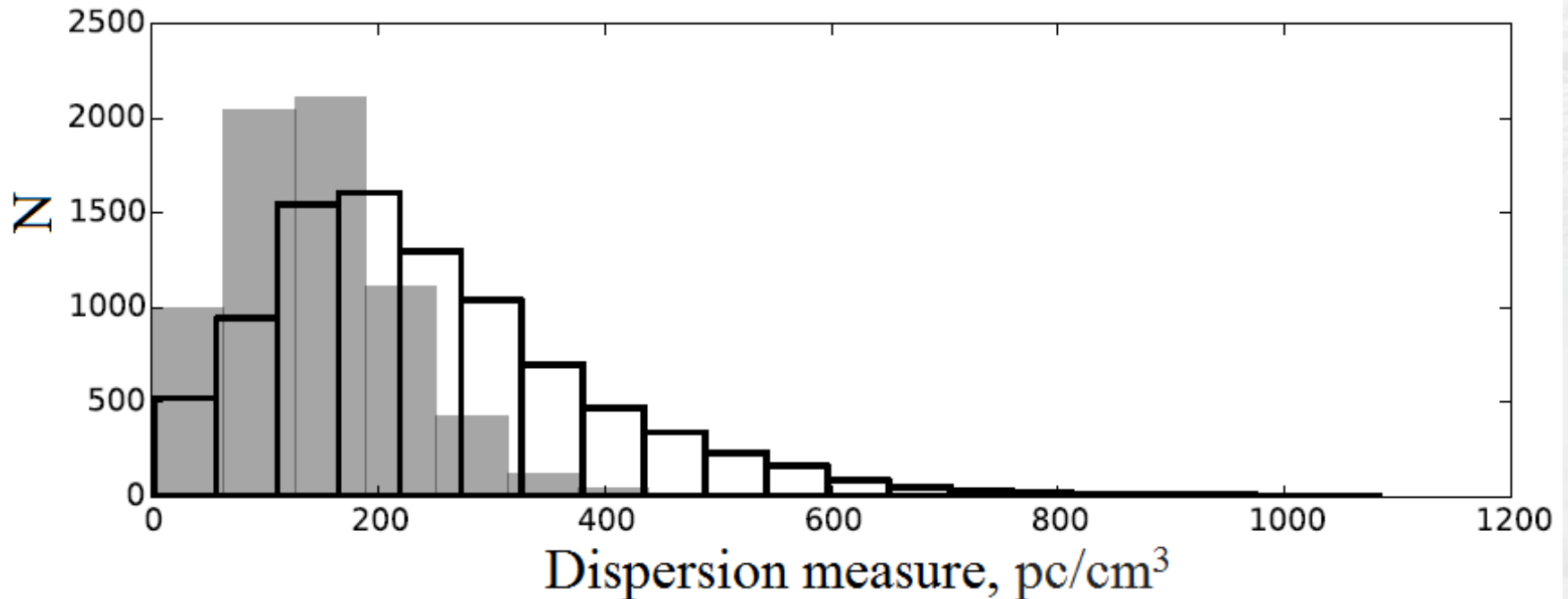
Histograms of the SNR distribution for signals with "direct" (top) and "inverse" DM (bottom)

380 events with SNR > 8

(O.M.Ulyanov, & V.V.Zakharenko 2012).

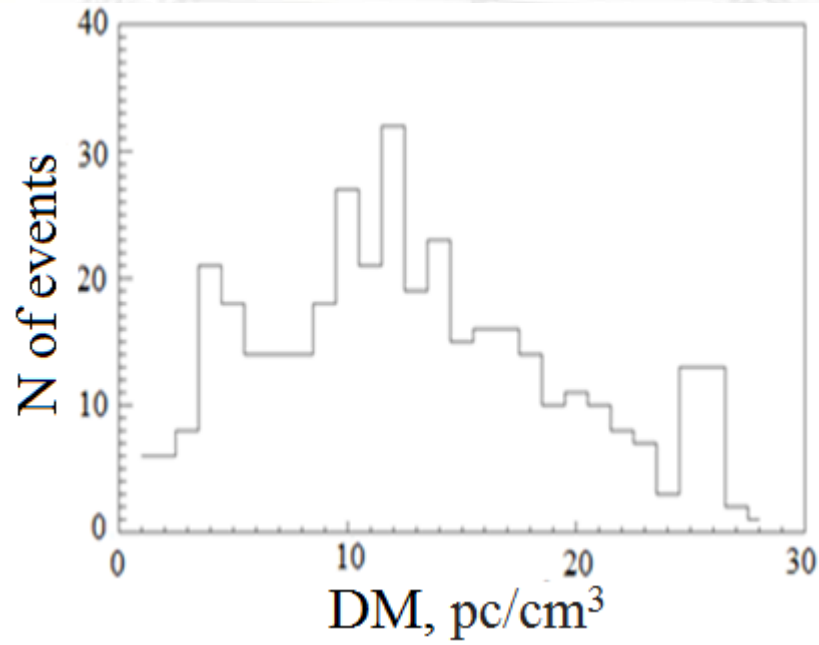


Simulated DM histogram of pulsars which will be available for observation at SKA radio telescope at 50-350 MHz (black bars) and 350+ MHz (clear bars)

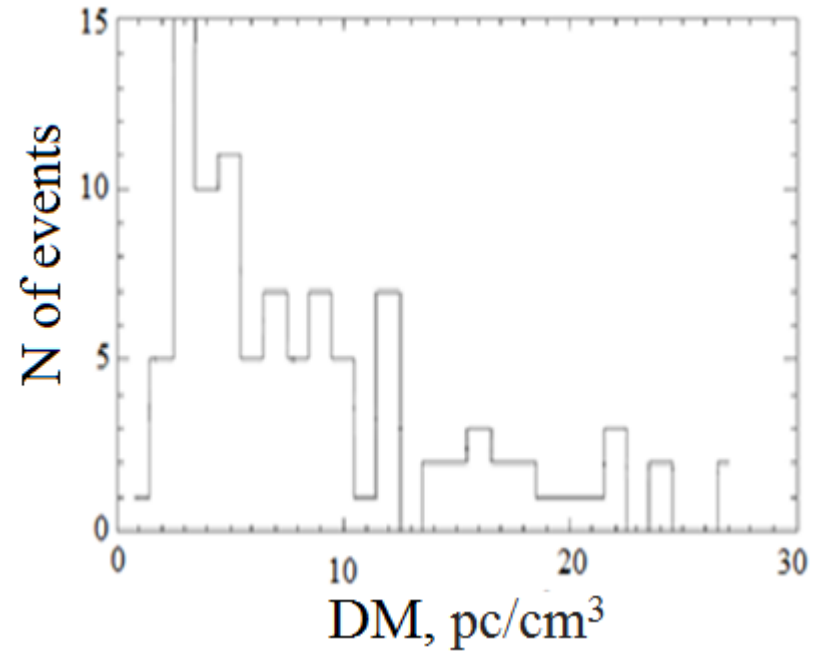
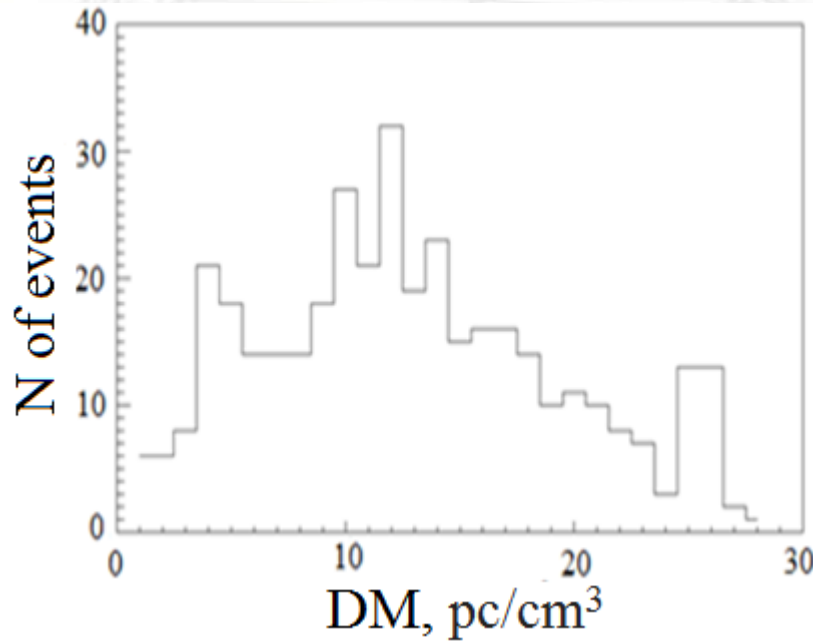


E. Keane et al., AASKA14, 2015

DMs' distribution of the signals with a "direct" DM (left)...

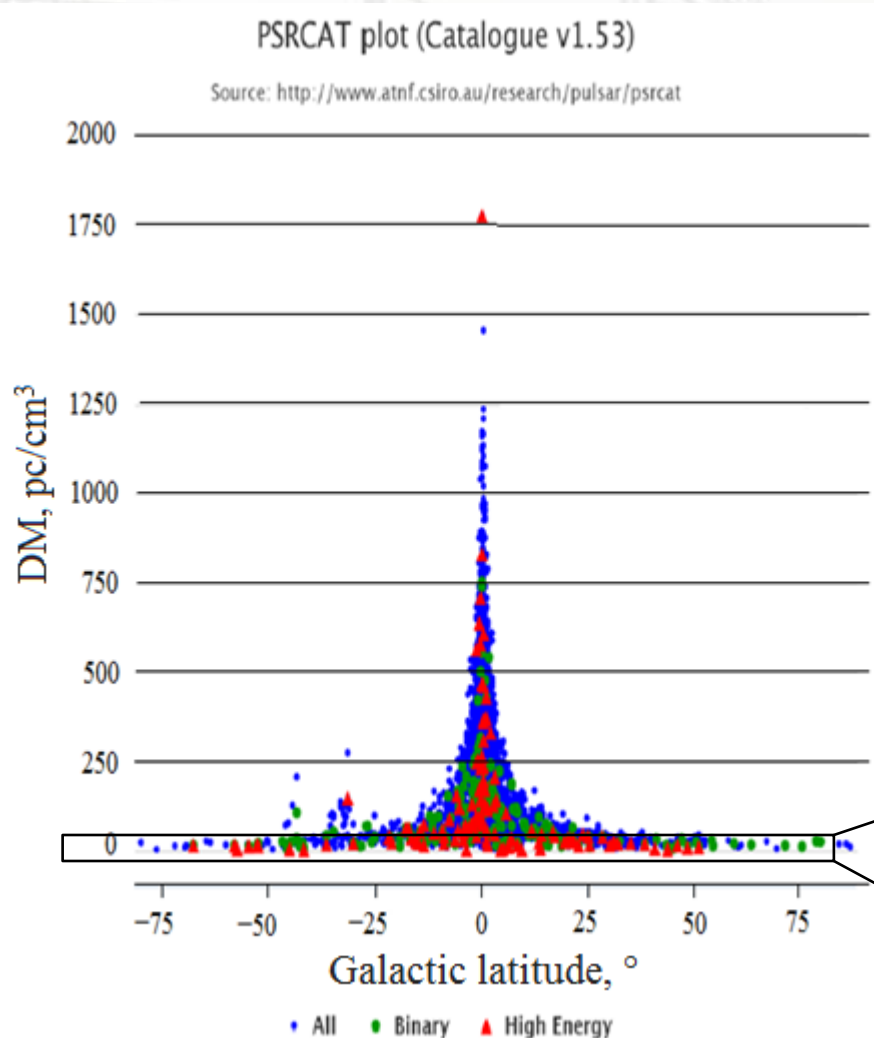


DMs' distributions of the signals with a “direct” DM (left) and “inverse” one (right)

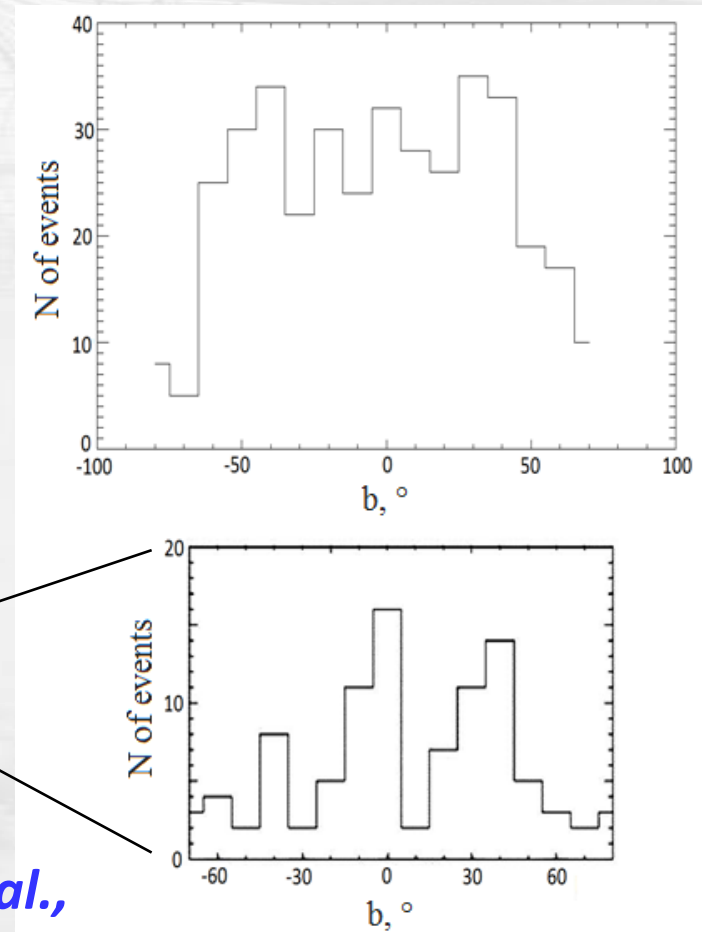


Left histogram is similar to the model from ([E. Keane et al., AASKA14, 2015](#)), but at the lower frequencies. Right panel shows the same histogram of the signals with “inverse” DM (100 events). It looks different. It's maxima is at low DM values (3 pc/cm³ – 15% of the total number). Only 25% of signals have DM = 10÷30 pc/cm³.

DMs' distribution of known pulsars from the ATNF catalog by galactic latitudes.



Galactic latitudes' distributions of signals found in the Survey (upper panel) and of close known pulsars (98 sources, DM < 30 pc/cm³ and P > 0.2 s) (lower panel)



*ATNF PSR Data Catalog: Manchester R. N. et al.,
ApJ, 2005*

Expected sources of radio emission:

- “Unfavorably” oriented pulsars at high frequencies;
- Rotating radio transients (RRATs);
- X-ray dim isolated neutron stars (XDINS);
- Anomalously intense pulses or giant pulses of MSP;
- Pulsars with a steep spectral indices (for example, -3) and therefore with reducing of the flux density at high frequencies (like PSR B0943+10);
- Some unknown sources both of cosmic and terrestrial origin.

Conclusions

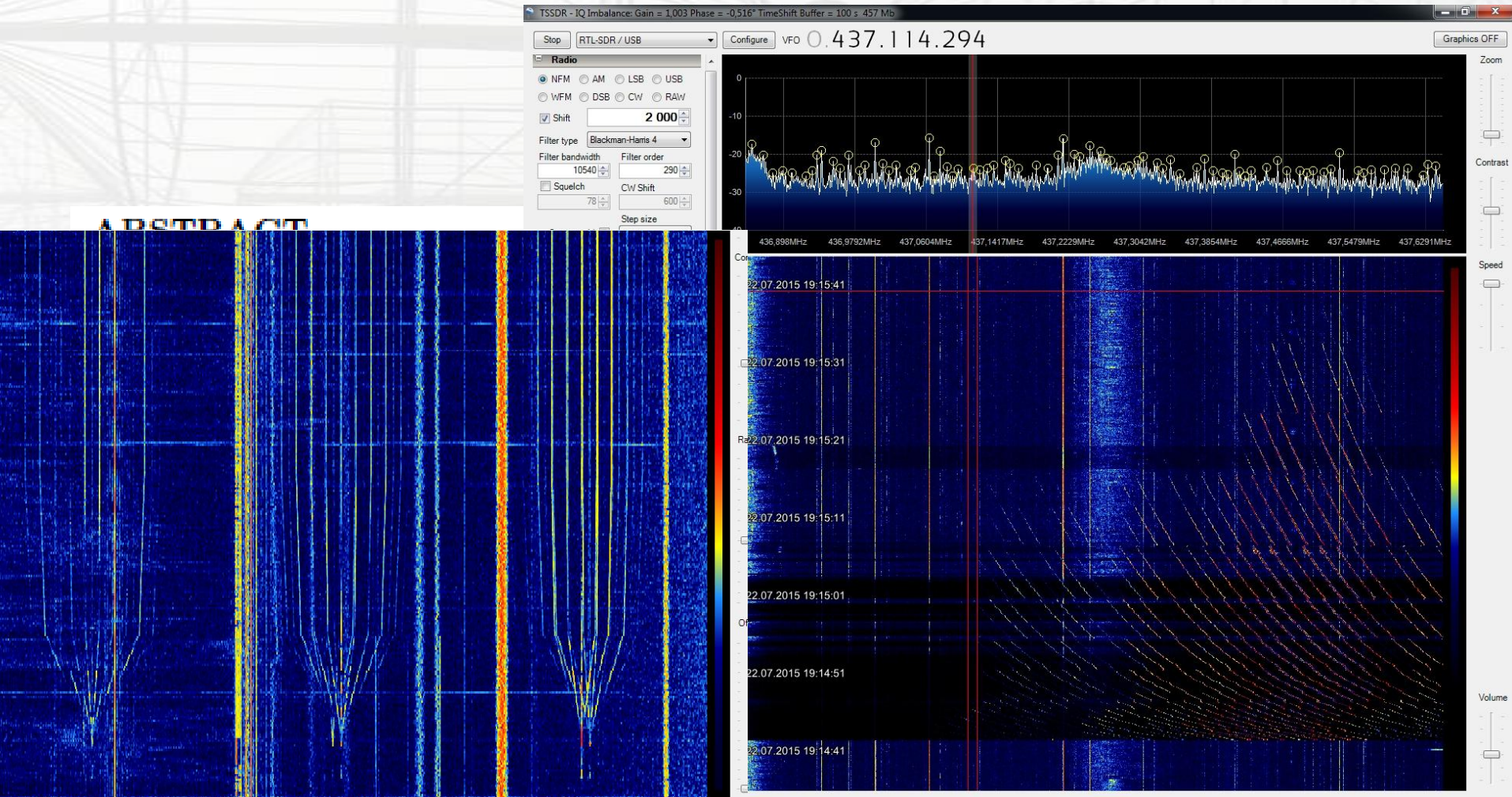
1. **380** transient radio signals with unique combination of DM and coordinates (so, 380 unique sources) were detected for the first time. Their parameters' distributions (of DMs and galactic latitudes) indicate a cosmic origin of these signals.
2. Using the developed “inverse” DM test, it was proved that these signals can't be explained by the ionospheric scintillation of cosmic continuous sources and also can not belong to some type of RFI, which have equiprobable distribution of leading or lagging low frequencies with respect to the upper ones.



**Thank you for
your attention !**

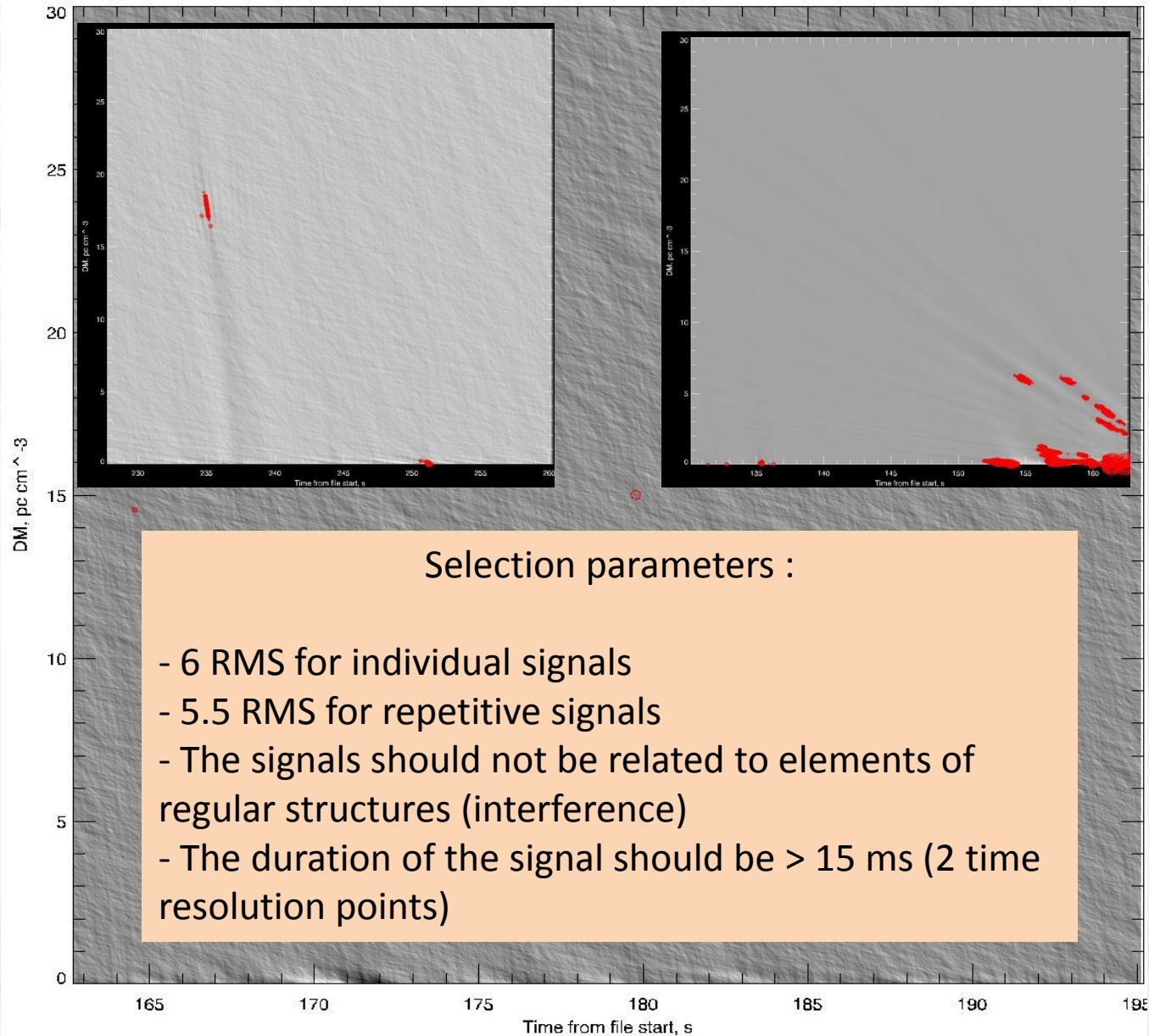


Поиск помех и выделение на их фоне космических сигналов (основная проблема обзора)



show that FRBs are excellent candidates for genuine extragalactic transients.

RFI structures



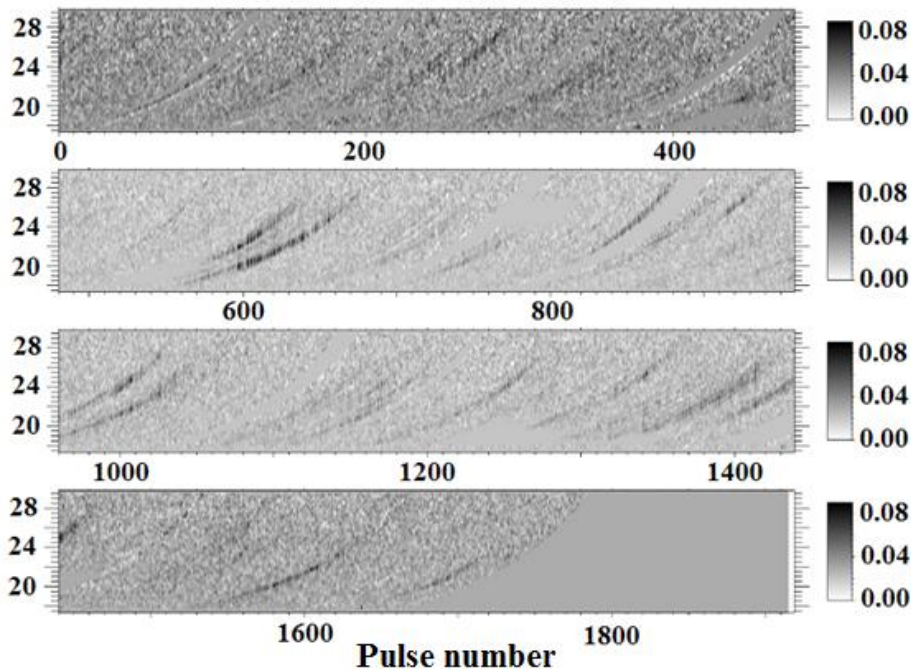
Влияние мерцаний

DM = 15.35

and

4.86 $\text{pc}\cdot\text{cm}^{-3}$

PSR B0943+10 25.02.2000



PSR B1133+16 29.03.2000

